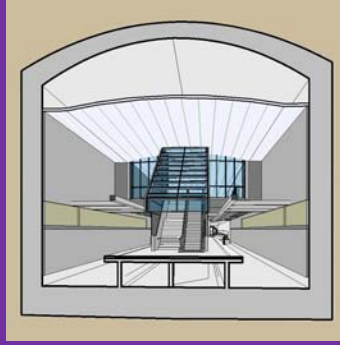


LOS ANGELES COUNTY METROPOLITAN TRANSPORTATION AUTHORITY
WESTSIDE PURPLE LINE EXTENSION PROJECT, SECTION 2
ADVANCED PRELIMINARY ENGINEERING

Contract No. PS-4350-2000



Probabilistic Fault Displacement Hazard Evaluation, Section 2

Prepared for:



Prepared by:

**PARSONS
BRINCKERHOFF**

777 South Figueroa Street, Suite 1100
Los Angeles, CA 90017

March 2017

Table of Contents

EXECUTIVE SUMMARY	ES-1
1.0 INTRODUCTION	1-1
1.1 Scope of Work.....	1-1
1.2 Previous and Ongoing Investigations.....	1-1
2.0 TECTONIC SETTING	2-1
2.1 Santa Monica Fault	2-1
2.1.1 Description and Regional Setting of the Santa Monica Fault	2-1
2.1.2 Uniform California Earthquake Rupture Forecast Models of the Santa Monica Fault	2-2
2.1.3 Potential for Multi-fault Ruptures	2-3
2.1.4 Results of Recent Investigations of the Santa Monica Fault	2-4
2.1.5 Location of Santa Monica Fault Crossings	2-5
2.2 Newport-Inglewood Fault.....	2-6
2.3 West Beverly Hills Lineament and Northern Extension of Newport-Inglewood Fault	2-7
2.4 Summary of Fault Activity for PFDHA	2-8
3.0 FAULT RUPTURE MODELS	3-1
3.1 Scenarios for Rupture of the Santa Monica Fault.....	3-1
3.2 Scenarios for Rupture of the Newport-Inglewood Fault	3-5
4.0 PROBABILISTIC FAULT DISPLACEMENT HAZARD ASSESSMENT	4-1
4.1 Methodology for Probabilistic Fault Displacement Hazard Analysis.....	4-1
4.1.1 Approaches for Frequency of Fault Displacement	4-1
4.1.2 Characteristic Earthquakes and Maximum and Average Fault Displacement....	4-1
4.1.3 Probability of Rupture along Alignment	4-2
4.1.4 Probability of Surface Rupture.....	4-2
4.1.5 Probability of Secondary Displacement.....	4-3
4.1.6 Selection of Primary versus Secondary Fault Displacement Models.....	4-3
4.1.7 Fault Displacement Models	4-4
4.2 Results of the PFDHA –Santa Monica Fault	4-4
4.2.1 Displacement Hazard for the Santa Monica Fault Rupture Scenarios.....	4-5
4.2.2 Mean Displacement Hazard for the Santa Monica Fault.....	4-6
4.2.3 Return Periods for Santa Monica Fault Displacement Exceedance.....	4-9
4.3 Results of the PFDHA –Newport-Inglewood Fault.....	4-9
4.3.1 Displacement Hazard for the Newport-Inglewood Fault Rupture Scenarios ...	4-10
4.3.2 Mean Displacement Hazard for the Newport-Inglewood Fault	4-10
4.3.3 Return Periods for Newport-Inglewood Fault Displacement Exceedance	4-12
4.4 Summary of Fault Displacement Parameters	4-12

5.0 LIMITATIONS 5-1

6.0 REFERENCES 6-1

List of Tables

Table 1: Fault Source Parameters from UCERF 3 Models 3-3

Table 2: Source Characteristics for Santa Monica Fault Rupture Scenarios 3-6

Table 3: Source Characteristics for Newport-Inglewood Fault Rupture Scenarios 3-8

Table 4: Santa Monica Fault rupture Scenario Parameters and Weights 4-6

Table 5: Mean Displacement Hazard for Santa Monica Fault 4-9

Table 6: Expected Return Periods for Displacement Exceedance – Santa Monica Fault 4-9

Table 7: Newport-Inglewood Fault Rupture Scenario Parameters and Weights 4-11

Table 8: Mean Displacement Hazard for Newport-Inglewood Fault 4-11

Table 9: Expected Return Periods for Displacement Exceedance – Newport -Inglewood Fault 4-12

List of Figures

Figure 1: Quaternary Faults and Geomorphic Features A-1

Figure 2: Regional Extent of Fault Sources A-2

Figure 3: Location of Quaternary Faults and UCERF 3 Fault Traces A-3

Figure 4: Fault Segments for Santa Monica Fault Rupture Scenarios A-4

Figure 5: Location of Modeled Fault Traces and Fault Crossings A-5

Figure 6: Santa Monica Fault Rupture Scenarios A-6

Figure 7: Newport-Inglewood Fault Rupture Scenarios A-9

Figure 8: Geometry and Displacement Model for Strike-Slip Faulting A-10

Figure 9: Santa Monica rupture Scenario Contributions and Total Mean Displacement Hazard A-11

Figure 10: Newport-Inglewood Rupture Scenario Contributions and Total Mean Displacement Hazard A-12

Executive Summary

A portion of the alignment of Section 2 of the planned Metro Westside Purple Line Expansion (WPLE) is in an area of Beverly Hills where mapped and inferred Quaternary traces of the Santa Monica fault and a northern extension of the Newport-Inglewood fault cross the tunnel alignment. To assess the potential impact of fault rupture to the tunnel, a probabilistic fault displacement hazard analysis (PFDHA) has been performed in accordance with the Metro Supplemental Seismic Design Criteria (Revision 9, 2015).

The fault traces utilized in the PFDHA were input to a computational model to evaluate the various potential scenarios for fault rupture that could affect the WPLE. The Uniform California Earthquake Rupture Forecast (UCERF) 2 (WGCEP, 2008) and UCERF3 (Field et al., 2013) include alternative models for the location and extent of faults. These models were used as a basis for the fault model used in the PFDHA. The fault model for the PFDHA considered an eastern extension of the South Trace of the Santa Monica fault that, based on field investigations, is slightly relocated from the UCERF3 model of this fault. The potential fault crossings of the South Trace in the PFDHA model were located along Tunnel Reach 5, which is the portion of the WPLE between the Wilshire/Rodeo Station on the east and the Century City Constellation Station on the west. A fault identified by Metro (2017) along Lasky Drive was presumed in the PFDHA fault model to represent the location of the eastward extension of the South Trace of the Santa Monica fault. An inferred northern extension of the Newport-Inglewood fault mapped by the California Geological Survey (2016) also may cross the subway tunnel alignment at Lasky Drive and was therefore included as part of the PFDHA fault model.

The Santa Monica fault is part of a series of generally east-west–trending active strike-slip and reverse faults that extend along the southern margin of the Transverse Ranges mountains from offshore of Santa Monica to the northeastern margin of the Los Angeles Basin. The Uniform California Earthquake Probabilities Forecast (UCERF) reports prepared by the Working Group on California Earthquake Probabilities (WGCEP, 2008) and by Field et al. (2013) show fault rupture models for combined ruptures along the offshore Anacapa Dume, Santa Monica, Hollywood, and Raymond faults, from west to east, as well as along other faults. These reports also include models for combined ruptures along the Rose Canyon, Offshore Newport-Inglewood, and Newport-Inglewood faults, from south to north, and extending northward along the West Beverly Hills Lineament (WBHL) or other northerly extension of the Newport-Inglewood fault to the Santa Monica, Hollywood, and other faults.

A series of fault scenarios that represent a range of reasonable potential combined ruptures along the Santa Monica fault and along a northern extension of the Newport-Inglewood fault was developed for potential fault crossings along Section 2 of the WPLE. The rupture lengths, rupture widths, and fault slip rates for the rupture scenarios are based on the models and data presented in the UCERF 3 report (Field et al., 2013). The expected displacements at the fault crossings are developed from a probabilistic fault displacement hazard analysis (PFDHA) as probabilities of exceedance of displacement, which are computed in a similar manner as a probabilities of exceedance of ground motion from probabilistic seismic hazard analysis (PSHA). The PFDHA was performed following the methodology of Youngs et al. (2003) and incorporates uncertainty in displacement based on alternative rupture lengths and widths for each rupture scenario and based on the minimum, best estimate, and maximum solution fault slip rates of UCERF3 (Field et al., 2013). The PFDHA also incorporates the probability that each possible rupture extends along the fault to the WPLE subway alignment and to the ground surface, following the methodology described in Youngs et al. (2003). The fault displacement was calculated using the bilinear regression model of Petersen et al. (2011) for average displacement at the ground surface given the

location of the fault crossing along the fault rupture, and the all-slip-type regression for average surface displacement from magnitude of Wells and Coppersmith (1994).

The expected displacement is calculated as a probability of exceedance of displacement (a displacement hazard curve) for selected return periods, including a 4 percent probability of exceedance (PE) in 100 years and a 50 percent PE in 100 years, which are approximately equivalent to a 2,450-year return period and 150-year return period, respectively. These displacement exceedance return periods correspond to the Maximum Design Earthquake (MDE) and Operating Design Earthquake (ODE) ground shaking exceedance levels, respectively, as specified in the Metro Supplemental Seismic Design Criteria (Revision 9, 2015).

The displacement hazard for the Santa Monica fault was evaluated from a series of 18 scenario ruptures that include multi-fault ruptures on the adjacent Anacapa Dume, Malibu Coast, Hollywood, and Raymond faults, and on two traces of the Santa Monica fault in the Beverly Hills area, the North Trace and the South Trace. Because both the North Trace and South Trace of the Santa Monica fault appear to be Quaternary- and Holocene-active, and because those traces are close to each other, it is possible that both faults may rupture during large earthquakes, and that displacement in a single earthquake event may be distributed along both faults. Of these two traces, the WPLE crosses the South Trace at Lasky Drive and also at Wilshire Boulevard. Given the location of the fault zone at Lasky Drive, and that exploration has not yet been performed to locate the nearby Wilshire Boulevard crossing, the PFDHA is performed for the fault crossing at Lasky Drive.

Based on available information, and specifically the field exploration and interpretations presented in Metro (2017), we assume that displacement during ruptures along the Santa Monica fault is distributed along both Santa Monica North and South Traces, with 75 percent of the displacement in each postulated rupture scenario occurring on the South Trace and 25 percent occurring on either the North Trace or in the area between the two traces of the Santa Monica faults. A mean displacement hazard curve was calculated from the weighted average of the 18 scenario ruptures to represent the displacement hazard for the Santa Monica South Trace at the Lasky Drive crossing. A mean hazard curve is the basic result of both probabilistic seismic hazard and probabilistic fault displacement hazard analyses, and presents the expected annual frequency of exceedance of various levels of ground motion or displacement, respectively. The weighting for the 18 individual scenarios was developed in consideration of the expected frequency of specific multi-fault ruptures, and an assessment of the probability that a rupture would continue to an adjacent fault.

A series of seven rupture scenarios were selected to represent a range of potential single and multi-segment ruptures on the Newport-Inglewood, Rose Canyon, Newport-Inglewood Offshore, Newport-Inglewood North Extension (NINE) and Hollywood faults. A common feature of the most likely rupture scenarios is that the fault crossing is close to the end of the ruptures, where the expected displacements are small. A mean displacement hazard curve for the Newport-Inglewood fault was calculated from the weighted average of four of the seven scenarios.

The expected surface displacement exceedance at Lasky Drive calculated from the mean displacement hazard curves for the Santa Monica fault (specifically the South Trace) and the Newport-Inglewood fault, for the ODE and MDE, is shown below.

Fault Rupture Scenario	Displacement Model	Return Period (years)	Expected Displacement Exceedance (cm)
Santa Monica South Trace – at Lasky Drive and also at Wilshire Blvd	Full PFDHA	150 (ODE)	<1
		2,450 (MDE)	13.0
Newport-Inglewood North Extension at Lasky Drive	Full PFDHA	150 (ODE)	< 1
		2,450 (MDE)	< 1

Displacement hazard results were calculated for additional fault scenarios to evaluate the sensitivity of the displacement to various input parameters and the empirical relationships used in the analysis. The results of these sensitivity analyses show that for the MDE, the results are sensitive to both fault slip rate and rupture length: increasing the input slip rate in the model results in an increase in computed displacement hazard, while increasing the input rupture length or magnitude in the model results in a decrease in hazard.

Based on the above results and sensitivity analyses, the fault displacement values for the tunnel may be taken as up to 1 centimeter (cm) for the same annual probability of exceedance as defined for ground shaking at the ODE level, and 13 cm for the same annual probability of exceedance as defined for ground shaking at the MDE level.

1.0 INTRODUCTION

This report presents the results of a site-specific probabilistic fault displacement hazard study performed by Amec Foster Wheeler Environment & Infrastructure, Inc. (Amec Foster Wheeler) for Section 2 of the Los Angeles County Metropolitan Transportation Authority (Metro) Westside Purple Line Extension (WPLE) subway in Beverly Hills, California. The Section 2 alignment extends from the Century City Constellation Station eastward to the west end of the Wilshire/La Cienega Station. The alignments for Sections 1 and 3 of the WPLE include the Wilshire/La Cienega Station and toward the east, and westward from the Century City Constellation Station, respectively. The reach of the Section 2 tunnel alignment between the Century City Constellation Station and the Wilshire/Rodeo Station is referred to as Reach 5. This reach is located in an area where traces of the east-northeast trending Santa Monica fault and the inferred north-northwest-trending northern extension of the Newport-Inglewood fault intersect. The planned subway alignment extends across possible Quaternary traces of these faults in several locations as shown in Figure 1.

1.1 Scope of Work

The primary objective of this study is to perform a probabilistic fault displacement hazard analysis (PFDHA) for locations where Section 2 of the WPLE crosses possible Quaternary faults and estimate the expected displacement for time periods corresponding to the Metro Supplemental Seismic Design Criteria (Revision 9, 2015) for the Maximum Design Earthquake (MDE) and Operating Design Earthquake (ODE). The MDE and ODE are defined at return periods of 2,500 years and 150 years (for ground motion exceedance), corresponding approximately to 4 percent probability of exceedance (PE) in 100 years, and 50 percent PE in 100 years, respectively. For this study, displacement exceedance is calculated for the MDE and ODE at the respective return periods of 2,500 and 150 years.

1.2 Previous and Ongoing Investigations

Amec Foster Wheeler previously investigated the locations of faults along Sections 2 and 3 of the WPLE (Metro, 2011), and in 2015 through 2016 performed additional investigations to constrain the nature, location, and activity of fault traces crossing both Sections 2 and 3 of the subway alignment (Metro 2016a, 2017). The analysis presented in this report is based primarily on data that were available as of February, 2017.

2.0 TECTONIC SETTING

A summary of geologic and geomorphic information regarding the location and activity of the Santa Monica and Newport-Inglewood faults based on information provided in Metro (2011, 2016a, 2016b, and 2017) and other studies is provided below.

2.1 Santa Monica Fault

The Santa Monica fault is part of a series of generally east-west–trending active strike-slip and reverse faults that extend along the southern margin of the Transverse Ranges mountains from offshore of Santa Monica to the northeastern margin of the Los Angeles Basin. The nature and setting of the fault, models for rupture on the Santa Monica fault, models for rupture of the Santa Monica fault with adjoining faults, results of recent investigations of the South Trace of the Santa Monica fault for the WPLE, and locations of WPLE crossings of the South Trace of the Santa Monica fault are described in the following sub-sections.

2.1.1 Description and Regional Setting of the Santa Monica Fault

The well-expressed geomorphic trace of the Santa Monica fault zone extends about 12.5 miles (20 km) westward from the western edge of Beverly Hills across West Los Angeles and Santa Monica to Pacific Palisades (Figure 1). The Santa Monica fault continues offshore and likely connects to offshore faults that extend west along the coastline to Point Dume and further westward (Figure 2; Santa Monica Offshore and Malibu Coast faults; Dolan and Sieh, 1992; Dolan et al., 1995; 2000), or west-southwest further offshore from Point Dume (Anacapa-Dume fault; Working Group on California Earthquake Probabilities [WGCEP], 2008). The Santa Monica fault zone exhibits both left-lateral and sub-ordinate reverse components of slip. The Santa Monica fault zone appears to connect northeastward to the west end of the Hollywood fault zone across a $\frac{3}{4}$ -mile (1.2 km) wide left-step, which occurs near or east of the northern part of the West Beverly Hills Lineament (WBHL), a northwesterly trending topographic rise present along the western boundary of the City of Beverly Hills (Figure 1 and Figure 3) (Dolan and Sieh, 1992; Dolan et al., 1997; 2000). The Hollywood fault zone extends from just east of the WBHL about 12 miles (19 km) east to another left step eastward on to the Raymond fault east of the Los Angeles River (Figure 4). In addition to the northern portion of the Santa Monica fault zone connecting to the Hollywood fault zone, the southern portion of the Santa Monica fault zone appears to extend east-northeast across the WBHL and along the southern margin of the Hollywood Basin, south of and subparallel to the Hollywood fault (FM 3.2 on Figure 3).

The Santa Monica and Hollywood fault zones are part of a much longer system of oblique left-lateral/reverse faults that form the more than 150-mile- (240-km-) long southern boundary of the Transverse Ranges (Figure 2). The Santa Monica fault system is related to the Pliocene-Quaternary structural development of the Santa Monica Mountains. Prior to the late Miocene, the Santa Monica Fault was a normal fault that was reactivated as a reverse fault beginning in the Pliocene (Tsutsumi et al., 2001). In the Century City area, Tsutsumi et al. (2001) interpreted the Santa Monica fault zone to consist of three southern strands and one northern strand, with only the northern strand being currently active. Other studies (Dolan et al., 2000; Dolan and Pratt, 1997; Hummon et al., 1992; Ziony et al., 1985) indicate that the northern strand of the Santa Monica fault zone is active and offsets or deforms Holocene sediments.

A prominent, north-side-up topographic scarp, as shown in Figure 1, can be traced continuously from the Los Angeles Country Club in Century City west to the mouth of Potrero Canyon in Pacific Palisades, where the Santa Monica fault zone extends offshore; the scarp marks the active strands of the Santa Monica fault zone through Century City, West Los Angeles, and Santa Monica (Dolan and Sieh, 1992, Dolan et al., 2000). This topographic scarp provides the most definitive geomorphic evidence for the approximate location of the surface expression of the Santa Monica fault zone, however, the specific locations and recency of activity of various fault strands that make up the zone have been determined at specific locations along the fault by detailed, site-specific studies such as described in Metro (2011, 2016a, 2016b, 2017), and other studies cited therein.

The continuity of the topographic scarp over the entire 7 mile (11.2 km) onshore length of the Santa Monica fault zone and paleoseismic data (e.g., Dolan et al., 2000) indicate that it is active, including the reach of the fault in the Century City area. As shown in Figure 1, the topographic scarp extends close to but does not extend east of the WBHL (Dolan et al., 2000; Dolan and Sieh, 1992). Rather, the easternmost part of the topographic scarp that defines the north trace of the Santa Monica fault diverges from Santa Monica Boulevard, assuming a more northeasterly trend through the Los Angeles Country Club east of Club View Drive and merges with the WBHL about $\frac{3}{4}$ mile (1.2 km) north of Santa Monica Boulevard, as shown in Figure 1. However, this eastern-most section of the topographic scarp appears to have been eroded by a southeastward-flowing drainage emanating from the main Benedict Canyon drainage to the east. Thus, although the scarp provides a robust northernmost possible location for a major trace of the north-dipping Santa Monica fault zone, the surface trace of the main, active strands of the Santa Monica fault responsible for generating the topographic scarp may lie somewhat to the southeast of the scarp, corresponding more closely with the location of Santa Monica Boulevard.

As described below, the WGCEP (2008) and Field et al. (2013) include two models for the location and extent of the eastern end of the Santa Monica fault, and consider that either model for the location and eastern extent of the fault may be active. A number of studies have evaluated surficial data, including topographic and geologic data, to assess the location and activity of one or more potential southern traces of the Santa Monica fault, such as modeled by Tsutsumi et al. (2001). Several of these studies, including Metro (2011, 2016a, 2016b, 2017); Leighton Consulting, Inc. (Leighton, 2012); and Olson (2015) identified faults in the area south of Santa Monica Boulevard and east of the WBHL, to confirm the existence of the South Trace of the Santa Monica fault. As described below (Section 2.1.4), studies by Metro (2017) provide evidence that the South Trace has ruptured multiple times during the latest Pleistocene and Holocene, thus, both traces of the Santa Monica fault are taken to be active.

2.1.2 Uniform California Earthquake Rupture Forecast Models of the Santa Monica Fault

The Uniform California Earthquake Rupture Forecast (UCERF) 2 (WGCEP, 2008) and UCERF3 (Field et al., 2013) include two alternative models for the location and extent of the Santa Monica fault. In Fault Model (FM) 3.1 of UCERF3, the Santa Monica fault extends along the topographic scarps over a length of 8.6 miles (14.4 km), from the vicinity of the WBHL westward, including a 1.5 mile (2.5 km) west-northwest extension along the offshore Santa Monica fault. In FM 3.2 of UCERF3, the Santa Monica fault extends eastward in the area immediately south of Santa Monica Boulevard, crossing the WBHL, and continuing about 7.6 miles (12.3 km) east-northeast subparallel to the Hollywood fault.

The FM 3.2 model trace for the Santa Monica fault lies just south of the corresponding FM 3.1 model trace in the Century City/west Beverly Hills area, as shown in Figure 3, and corresponds generally to the

location of the buried southern trace of the Santa Monica fault as mapped by Tsutsumi et al. (2001). The eastern extent of this FM 3.2 model trace appears to be approximately aligned with the east-northeast-trending southern margin of the Hollywood Basin and the North Salt Lake fault as mapped by Hill et al. (1979), Wright (1991), and Hildenbrand et al. (2001). The western reach of the FM 3.2 model trace for the Santa Monica fault steps northward near Bundy Drive, and continues westward along topographic scarps and then offshore, with a dog-leg to the southwest in the offshore region to approach the east end of the offshore Anacapa-Dume fault as shown in Figure 2 and Figure 3. The FM 3.2 model for the Santa Monica fault has a total length of 17.5 miles (28 km).

A comparison of the mapped Quaternary faults (US Geological Survey, 2014) and the UCERF fault models (WGCEP, 2008; Field et al., 2013) is shown on Figure 3. Other inferred faults mapped by the California Geological Survey (CGS, 2016; Olson, 2015; Treiman et al., 2015) also are shown on Figure 3. On this figure, the North Salt Lake fault represents the buried fault that forms the south margin of the Hollywood Basin, but we note that the location of this bounding fault and the southern margin of the Hollywood Basin differs somewhat among the various authors cited above. We also note that there are no distinct topographic scarps to demark the potential surface expression of the South Trace of the Santa Monica fault east of the WBHL and South Moreno Drive.

The UCERF2 and UCERF3 fault models were developed for the explicit purpose of calculating the probabilities of future earthquakes in California and the resulting ground motions. The fault traces are somewhat generalized or simplified for use in a PSHA, and may not be exactly coincident with the mapped or inferred location of the actual fault at the ground surface at some locations. Therefore, although UCERF2 and UCERF3 are useful for a PSHA and for general location of faults in a PFDHA, a more precise location of fault traces near a project site needs to be considered to perform a PFDHA. For this assessment, the location of the Santa Monica fault has been refined to more closely match the location of the surface traces of the fault, and in the area of the WPLE crossings, the PFDHA model of the fault was placed at the center of the fault zones identified in Metro (2011, 2016a, 2017).

Although no large magnitude historical earthquakes (greater than about M 5.0) are associated with the Santa Monica or Hollywood faults (Southern California Earthquake Data Center [SCEDC], 2016), the faults are considered capable of generating earthquakes of M 6.7 or larger as described in the UCERF studies (WGCEP, 2008; Field et al., 2013).

2.1.3 Potential for Multi-fault Ruptures

A critical issue in assessing the size of earthquakes that may cause surface rupture along the WPLE alignment is the potential for continuity of ruptures across various faults that form the southern boundary of the Transverse Ranges. The most recent assessment of probabilities of earthquakes for UCERF3 allows for extensive multi-fault ruptures, extending along many faults over hundreds of kilometers, but these long ruptures typically have very low recurrence rates, on the order of 10's to 100's of thousands of years (Field et al., 2013). The WGCEP (2008) indicates the Santa Monica fault may rupture with the Anacapa-Dume fault in earthquakes of up to M 7.6, while Field et al. (2013) indicate the Santa Monica fault may participate in multi-fault ruptures with earthquakes of up to M 8.0.

For this study, the likelihood of ruptures extending over adjoining faults such as the Anacapa Dume, Malibu Coast, Santa Monica, Hollywood, and Raymond faults was assessed based on review of the frequency of participation of the Santa Monica fault with adjoining fault segments as shown in UCERF3 (Field et al., 2013) and was also assessed based on the observed continuity of fault traces, similarity of

geomorphic expression of faulting, the recency and timing of past ruptures, similarity of slip type, continuity of seismicity, continuity of faults in the subsurface, and other factors. The available information on the nature of and mapping of these faults indicates that ruptures may extend across two or more of the Anacapa Dume, Malibu Coast, Santa Monica, Hollywood, and Raymond faults (Dolan et al., 1995, 1997, 2000; Weaver and Dolan, 2000), with rupture lengths ranging from approximately 5 to 46 miles (9 to 75 km).

Additionally, because the UCERF models include ruptures along faults with mid to latest Pleistocene and Holocene activity (i.e., those that have ruptured in the past 780 thousand years [ka]), not all faults in the UCERF models represent a hazard for surface rupture as defined by the Alquist Priolo Act (restricted to faults that are known to have ruptured during the Holocene [past 11 ka]) or by other criteria for fault activity extending over longer time periods to 30 ka or 40 ka. Because Holocene activity has been confirmed on the Santa Monica, Hollywood, Raymond, and Malibu Coast faults, and late Quaternary activity has been confirmed for the Anacapa-Dume fault (Dolan et al., 1997, 2000; Weaver and Dolan, 2000; Jennings and Bryant, 2010), for this PFDHA it is reasonable to consider the potential for ruptures to occur across any combination of these faults that include the Santa Monica fault.

2.1.4 Results of Recent Investigations of the Santa Monica Fault

Subsurface explorations, including trenches, test pits, soil borings, and cone penetration tests (CPTs), have been performed in the area of Century City and west Beverly Hills and provide information regarding traces of the Santa Monica fault and faults associated with the Newport-Inglewood fault system (e.g., Metro, 2011, 2016a, 2016b, 2017; Leighton Consulting, Inc. [Leighton], 2012, 2016; Geocon West, Inc., 2013, 2014). Specifically, surficial evidence for the presence of the South Trace of the Santa Monica fault was observed as far east as Moreno Drive in Beverly Hills in Trench 5 and Borings CB-23, CB-24, and CB-26 of Leighton (2012) and Transect 7 of Metro (2011). Additional information regarding the potential presence of a fault east of Moreno Drive corresponding approximately to the location of the South Trace of the Santa Monica Fault (FM3.2) includes an inferred fault mapped by the California Geological Survey (Olson, 2015) along a groundwater barrier over a distance of nearly one mile (1.5 km) east from the WBHL, and the fault bounding the south side of the Hollywood Basin as described in Section 2.1.2 (Figure 3).

The results of subsurface explorations performed by Amec Foster Wheeler along Section 2 and Section 3 of the WPLE in 2015 to 2017 provide strong evidence for the presence of the South Trace of the Santa Monica fault at Lasky Drive, as well as evidence for multiple late Pleistocene-Holocene surface ruptures on the South Trace of the Santa Monica fault. The 2015-2017 investigations (Metro, 2016a, 2017) included a series of closely spaced soil borings and CPTs in transects along Beverly Glen Boulevard and Benecia and Comstock Avenues to supplement similar explorations previously performed for transects extending along Century Park West, Avenue of the Stars, and Moreno Drive (Metro, 2011; Geocon West, 2013). The data along these transects were used to define stratigraphic horizons in profiles that show clear down-to-the-north and down-to-the south offsets of the top of the San Pedro Formation, forming a down-dropped graben that defines the location of the major traces of the Santa Monica fault in Century City and Beverly Hills.

At Lasky Drive in Beverly Hills, the latest Pleistocene and Holocene sediments are significantly thicker where they overlie the offset (down-dropped) top of the San Pedro Formation (Metro, 2017). This thick section of latest Pleistocene to Holocene sediments is interpreted to represent infilling of a structural

trough/ponding of sediments against the southern margin of a fault-bounded basin, and confirms the presence of the South Trace of the Santa Monica fault at Lasky Drive (Metro, 2017).

The apparent vertical offset of the top of the San Pedro Formation appears to be of about the same order of magnitude across multiple transects extending across the South Trace of the Santa Monica fault, from Beverly Glen Boulevard (Transect 6) on the west to Lasky Drive (Transect 9) on the east (as shown in Metro, 2016a, 2017), and is consistent with an interpretation that the South Trace of the Santa Monica fault could extend further east-northeast from Lasky Drive and approximately along the southern edge of the Hollywood Basin. Based on the apparent tectonic control of latest Pleistocene and Holocene sedimentation in the area of Lasky Drive, it appears that one or more rupture(s) have extended along the South Trace of the Santa Monica fault in the latest Pleistocene and Holocene. Because the apparent vertical offset of the top of the San Pedro Formation west of the convergence of the North and South Traces of the Santa Monica fault in Century City, and the displacement to the east along the South Trace of the Santa Monica fault at Lasky Drive in Beverly Hills is about the same order of magnitude, it therefore appears that the larger portion of Quaternary surface displacement on the Santa Monica fault has occurred along the South Trace of the fault. For this evaluation for Section 2 of the WPLE, we assess the potential for fault displacement on both the North Trace and South Trace of the Santa Monica fault.

2.1.5 Location of Santa Monica Fault Crossings

The most critical input to the PFDHA evaluation is the location of fault crossings of the subway alignment. Of the UCERF3 fault traces (FM 3.1 and FM 3.2), only the South Trace (FM3.2) extends across Section 2 of the WPLE subway tunnel as shown on Figure 3. Subsurface investigations by Metro (2011, 2016a, 2017) further refine the location of the southern portion of the Santa Monica fault zone as being along the south side of Santa Monica Boulevard in Century City, from west of Beverly Glen Boulevard continuing east-northeast. The model of the South Trace crosses Wilshire Boulevard west of the Wilshire-Rodeo Station (Figure 45). Because of the relatively narrow width of faulting identified by Metro along Santa Monica Boulevard (2011, 2017) west of Constellation Boulevard, the North and South Traces of the Santa Monica fault are considered to be coincident west of Section 2 of the WPLE. The change in trend of the topographic scarp and subsurface explorations by other consultants (described in Metro, 2016b), show that the North Trace of the Santa Monica fault diverges northeast through the Los Angeles Country Club north of Santa Monica Boulevard, while the South Trace of the Santa Monica fault continues east-northeast on the south side of Santa Monica Boulevard (Figure 1 and Figure 45).

The fault-bounded structural trough identified crossing Lasky Drive by Metro (2017) constrains the location of the South Trace of the fault where the alignment of the WPLE extends across the fault near Lasky Drive. For the purpose of the model, the South Trace is assumed to continue east along the same trend to cross the WPLE at Wilshire Boulevard (Figure 5). No subsurface investigations have yet been performed to specifically constrain the fault's orientation east or north of Lasky Drive, however data available to date indicates that there is not a fault crossing east of the west end of the Wilshire/Rodeo Station. Given the assumed strike of the fault east of Lasky Drive, the distance from the observed location of the fault at Lasky Drive to the eastern-most crossing of the WPLE at Wilshire Boulevard is on the order of 0.3 miles (0.5 km) (Figure 5). In the context of performing a PFDHA, given this close proximity, and that the modeled Santa Monica and adjoining faults extend for many miles east and west of these crossings as shown on Figure 4, the expected displacement would not be significantly different for these two potential crossings of the WPLE in Section 2.

2.2 Newport-Inglewood Fault

As mapped by the California Geological Survey (CGS 2010, 2016), the Newport-Inglewood fault zone comprises a series of discontinuous left-stepping strike slip fault traces that extend north-northwest for about 40 miles (65 km) across the Los Angeles Basin from Newport Beach, through the Cheviot Hills, and possibly extending further north-northwest. The south end of the fault zone continues on a south-southeast trend from Newport Beach in the offshore region for about 41 miles (66 km), and appears to connect to the Rose Canyon fault across a right step south of Oceanside. The Rose Canyon fault extends about 47 miles (75 km) south-southeast and south onshore through La Jolla and San Diego and offshore toward the International Border, as shown on Figure 2.

Two equally weighted alternatives for the location of the Newport-Inglewood fault are presented in WG08 and UCERF3, FM 3.1 and FM 3.2 of UCERF3, respectively. These modeled faults are both about 65 km long, extending south-southeast from about 0.6 mile (1.0 km) north of the Santa Monica Freeway (Interstate 10) in Beverly Hills, to the coast in Newport Beach. The north end of the UCERF model traces extend about 1.2 miles (2.0 km) northwest of the northern extent of the mapped surface traces of the fault in the Baldwin Hills. At the south end, the fault steps right in the offshore area along the coast to the Newport-Inglewood Offshore fault (Figure 2). Although the fault has been mapped in detail and has been identified in numerous fault trenching investigations for building and other structure development projects, little geologic data has been developed to directly assess the late Quaternary to Holocene slip rate of the fault. The current estimates indicate that the fault slip rate is on the order of 1 mm/yr (Field et al., 2013). The geomorphic expression of the fault and earthquake data indicate that the fault is characterized by right-lateral strike slip motion.

The locations of the alternative UCERF3 onshore traces of the Newport-Inglewood fault (FM 3.1 and FM 3.2) are different over several portions of the fault south of Interstate 10, but are coincident at the north end of the fault (Figure 3). We note that because the difference in fault lengths is small between these alternative locations, and because the areas where the model traces are different are not near the WPLE, the uncertainty in fault location has no effect on the evaluation of displacement at the subject evaluation area north of the end of the UCERF3 model fault traces. Therefore, we use the UCERF3 trace and rupture parameters for the Newport-Inglewood FM 3.1 fault as representative of the location and geometry of the Newport-Inglewood fault, with the exception of the more detailed trace location modeling near the subject evaluation area.

The Newport-Inglewood Offshore fault extends southeast along the coast about 41.5 miles (66.5 km) from Newport Beach in Orange County to offshore of Oceanside in northern San Diego County (Figure 2). There is a small 0.9 mile (1.5 km) right step between the southern end of the Newport-Inglewood Offshore fault and the northern end of the Rose Canyon fault; as this step is relatively small, it is not considered to represent a barrier for ruptures to propagate along both faults in a large earthquake. The Rose Canyon fault continues south-southeast about 47 miles (75 km), extending onshore at Mount Soledad in La Jolla, and continuing south-southeast to San Diego Bay (Figure 2).

The UCERF3 model for ruptures along the Newport-Inglewood fault (Field et al., 2013) shows that the Newport-Inglewood fault is most likely to participate in ruptures with the Newport-Inglewood Offshore and Rose Canyon faults over rupture lengths up to about 130 miles (210 km). The UCERF3 model shows that the Newport-Inglewood may participate in ruptures across the Santa Monica fault and faults to the

west, but much less frequently than for participation with the Newport-Inglewood Offshore and Rose Canyon faults.

In 1933, the southern Los Angeles basin section of the Newport-Inglewood fault zone ruptured to produce the M 6.4 Long Beach earthquake. The rupture did not reach the ground surface, but is inferred to have extended for 8 to 10 miles (13 to 16 km) based on the distribution of aftershocks (Hauksson and Gross, 1991). Although no large historical earthquakes have occurred along the fault north of Long Beach (SCEDC, 2016), the seismic hazard from the northern section of this major fault system in the Los Angeles region has been long known. For example, the California Division of Mines and Geology (now the California Geological Survey [CGS]) chose to model a hypothetical M 7.0 earthquake on the northern Newport-Inglewood fault zone as one of their first non-San Andreas earthquake scenarios (Topozada et al., 1988). The WGCEP (2008) indicates the Newport-Inglewood may rupture with the Newport-Inglewood Offshore and Rose Canyon faults, generating earthquakes of up to M 7.75, while Field et al. (2013) indicate that the Newport-Inglewood fault may participate in multi-fault ruptures with earthquakes of up to M 7.9. The location of the northern-most extent of the Newport-Inglewood fault zone is uncertain. While the northern-most well-defined surface traces extend slightly north of the Baldwin Hills (Figure 3), several workers studies have suggested that the fault continues northward to intersect the Santa Monica and Hollywood faults in the vicinity of the West Beverly Hills Lineament as described below.

2.3 West Beverly Hills Lineament and Northern Extension of Newport-Inglewood Fault

The WBHL is an approximately 3.4-mile (5.5 km) long north-northwest-trending topographic feature that extends through the area from north of Interstate 10 to north of Sunset Boulevard, and that crosses Santa Monica Boulevard east of the Century City – Constellation Station in the vicinity of South Moreno Drive (Figures 1, 3, and 5). The WBHL marks a pronounced boundary between uplifted and highly dissected older sedimentary units to the west and a gently sloping, younger alluvial plain in Beverly Hills to the east. Identified by Dolan and Sieh (1992) and Dolan et al. (1997; 2000) based on this pronounced topographic dissimilarity, the lineament is characterized by a discontinuous series of east-facing topographic scarps. These scarps have been eroded and modified by the south-flowing drainage emanating from Benedict Canyon (Figure 1).

Various tectonic interpretations have been proposed for the WBHL as described in Metro (2011), and field investigations have been performed at several locations along the WBHL to assess the presence or absence of faults, and the nature and recency of any faults that were identified. To the north of its intersection with the North Santa Monica fault zone, the WBHL was previously thought to act as a connection between the Santa Monica and Hollywood fault zones, transferring slip between these two strike-slip/oblique-slip fault systems (Figures 1 and 3; Dolan and Sieh, 1992; Dolan et al., 1997; 2000; Field et al, 2013). Dolan et al. (1997) speculated that this northern part of the WBHL might represent an east-dipping normal fault associated with extension along the left step between these faults. To the south of its intersection with the Santa Monica fault zone, Dolan and Sieh (1992) and Dolan et al. (1997; 2000) considered the WBHL to be the northern continuation of the active Newport-Inglewood fault zone located approximately 3 miles to the south-southeast as shown on Figure 3 and Figure 5.

By virtue of its assumed connection to the active Newport-Inglewood fault zone, the WBHL is considered by the USGS and CGS to be a latest Pleistocene-Holocene fault as shown in the U.S. Geological Survey

Quaternary Fold and Fault database (Bryant, 2005; USGS and CGS, 2010). UCERF3 (Field et al, 2013) models possible ruptures of the Newport-Inglewood fault as extending along the WBHL to connect to the Santa Monica and other faults. However, a fault investigation performed for Beverly Hills High School by Leighton (2012) did not identify a significant north-trending fault on the school campus at the location of the WBHL shown by the USGS and CGS (Bryant, 2005, USGS and CGS, 2010). Thus, the WBHL does not appear to represent the location of an active north-northwest-trending fault. The investigation by Leighton (2012) did not extend east of the campus and recent studies by the CGS (CGS, 2016 and Treiman et al., 2015) interpreted the northern extension of the Newport-Inglewood fault zone to be east of the WBHL. The revised Los Angeles 30 x 60 Quadrangle 1:100,000 scale geologic map (CGS, 2016) shows a two-mile (3.2-km) long inferred fault that extends approximately north-northwest subparallel to and east of the WBHL (shown as the CGS (2016) inferred fault trace on Figure 3). Metro's recent investigation (2017) identified faulting in the area of Lasky Drive, generally coincident with the location of the CGS (2016) inferred fault, although the strikes of all of the identified fault traces are not well constrained, and that faulting may instead be associated with the South Trace of the Santa Monica fault.

Treiman et al. (2015) used LiDAR imagery to identify linear topographic features that they speculate correspond to an active fault representing a northward extension of the Newport-Inglewood fault. The southern end of this inferred trace lies about 0.3 miles (0.5 km) east of the north end of the FM3.1 trace of the Newport-Inglewood fault and extends for 1.5 km north-northwest. The northern end of this inferred fault lies about 0.5 miles (0.8 km) south-southeast of the Wilshire-Rodeo Station along Wilshire Blvd. Other than the inferred fault mapped by CGS (2016), we are not aware of any other information regarding the possible extent or presence and activity of faults that may represent a northern extension of the Newport-Inglewood fault to cross the WPLE along Wilshire Blvd.

2.4 Summary of Fault Activity for PFDHA

Following the standard of practice in performing PSHA, the PFDHA performed for this project considers all faults with known or suspected Quaternary activity that may intersect or that could cause tectonic deformation to Section 2 of the WPLE. As described above, Section 2 of the WPLE extends across the modeled South Trace of the Santa Monica fault in Beverly Hills, with crossings along Lasky Drive and Wilshire Boulevard (Figure 5), and the South Trace has known latest Pleistocene to Holocene activity. The northern extent of mapped surface traces of the Holocene active Newport-Inglewood fault lie about 2.6 to 2.9 miles (4.2 to 4.7 km) south of the WPLE in the Century City-Beverly Hills Area. A possible northern extension of the Newport-Inglewood fault such as mapped by CGS (2016) would cross the WPLE in the vicinity of Lasky Drive (Figure 5). Therefore, based on CGS (2016), we assume that ruptures on the Newport-Inglewood fault may extend northward along a north-northwest-trending fault east of the WBHL and Beverly Hills High School, would cross Lasky Drive in the fault zone identified in Metro (2017), and would extend north to the Hollywood fault as shown on Figure 5.

Faults that have no evidence for Quaternary activity are considered not-active, and are not included in the PFDHA. Other Quaternary faults that are buried and do not extend to the surface or depth of the subway tunnel, and that are not known to have caused tectonic deformation such as folding or tilting in the near-surface in the area of the WPLE, such as the Puente Hills, Elysian Park Lower, and San Vicente faults (Figure 3), do not represent a potential surface rupture or surface deformation hazard to the WPLE. Therefore, these buried faults are not considered in the PFDHA.

In summary, based on review of published mapping of the recency of fault activity (Jennings and Bryant, 2010 and CGS, 2016), assessments of potential for fault rupture and strong ground shaking (WG08; Field et al., 2014; Peterson et al., 2014), and investigations of the location and activity of possible traces of the Santa Monica fault and northern Newport-Inglewood fault (Metro, 2011, 2016b, 2017; and Kenney Geoscience, 2014), no faults other than the South Trace of the Santa Monica fault and a possible northern extension of the Newport-Inglewood fault are known that may result in surface rupture or surface deformation hazard for Section 2 of the WPLE.

3.0 FAULT RUPTURE MODELS

The information necessary to perform a PFDHA is similar to that necessary to perform a PSHA, including the location, extent, and frequency of earthquakes on a fault, but only those faults that lie in immediate proximity to the structure of concern need be considered for a PFDHA. As noted in Section 2 of this report, mapped or inferred traces of the Santa Monica and Newport-Inglewood faults may underlie Section 2 of the WPLE, and potential ruptures of these faults are considered in the PFDHA. The specific scenarios and rupture parameters for those scenarios are described in this section.

The rupture scenarios for the PFDHA are selected from rupture scenarios for the Santa Monica and the Newport-Inglewood faults described for UCERF2 (WGCEP, 2008) and UCERF3 (Field et al., 2013), and include combined or extended ruptures along adjacent fault segments. These rupture scenarios for the PFDHA are modified from the published scenarios based on site-specific data from investigations of the Santa Monica fault and WBHL in the Century City area of Los Angeles. Additional information and the methodology and fault displacement models used in the PFDHA, and the results of the PFDHA are described in Section 4.

3.1 Scenarios for Rupture of the Santa Monica Fault

Rupture scenarios for the Santa Monica fault are based on models presented by WGCEP (2008), UCERF3 (Field et al., 2013), and additional published and unpublished data. These rupture scenarios for the PFDHA include combined or extended ruptures along adjacent fault segments, and are modified from the UCERF models based on site-specific data from investigations of the Santa Monica fault and WBHL in the Century City area of Los Angeles and additional published data.

As described in Section 2.1, two equally weighted alternatives for the location and eastern extent of the Santa Monica fault are presented in WG08 and UCERF3, FM 3.1 and FM 3.2 of UCERF3, respectively. For FM3.1, the North Trace, the east end of the Santa Monica fault is aligned along the mapped topographic scarp extending northward from Santa Monica Boulevard to Wilshire Boulevard, as shown on Figure 1, and corresponding to the mapped Quaternary fault trace as shown on Figure 2 and Figure 3 (USGS, 2014). For FM3.2, the South Trace, the eastern reach of the Santa Monica fault lies slightly south of the topographic scarps and Santa Monica Boulevard (as shown on Figure 3), extends east-northeast across the WBHL and continues subparallel to the Hollywood fault over a distance of about 7.4 miles (12 km) (Figure 3). As described in Section 2.1.2, the UCERF3 models for the Santa Monica fault are adopted and modified for use in this study, specifically by revising the location of the fault to closely follow the mapped surface extent of the fault west of Century City and in Beverly Hills, and to the center of the location of the fault zone, North Trace or South Trace, at the locations of the fault zone identified in Metro (2011, 2016a, 2017).

Based on the presence of the buried faults along the Hollywood Basin, as well as the relatively large and consistent offset of stratigraphic deposits (top of San Pedro Formation) noted in Leighton (2012), Transect 7 (Metro, 2011), and Transect 9 (Metro, 2017), it appears that the South Trace of the Santa Monica fault could extend for some distance east of Lasky Drive such as shown by Olson (2015), and likely farther east along the southern edge of the Hollywood Basin as shown by the UCERF2 and UCERF3 models (Figure 34). Therefore, for the location of the South Trace of the Santa Monica fault (FM3.2) east of the crossing of the WPLE at Wilshire Boulevard, the modeled trace is extended along the southern margin of the Hollywood Basin to the eastern end of the basin, a distance of 5.9 miles (9.4 km). The

location of the South Trace east of Wilshire Boulevard is based on the extent of the basin mapped by Wright (1991), Hummon et al. (1994), and Hildenbrand et al. (2001), and the location of the North Salt Lake fault or other faults bounding the south side of the Hollywood Basin mapped by Hill (1979), Wright (1991), Hildenbrand et al. (2001), Tsutsumi et al. (2001), and Field et al. (2013). The location of the modified South Trace of the Santa Monica fault is shown on Figure 4, and is referred to as the Santa Monica South trace. Although there is no distinct topographic scarp or other surficial expression characteristic of active faulting along an eastward projection of the South Trace of the Santa Monica fault, such as is observed along the Santa Monica fault west of the WBHL and along the Hollywood fault east of the WBHL, it is likely that past scarps formed by fault rupture have been buried by late Pleistocene and Holocene alluvial deposition. The Santa Monica South Trace (Santa Monica South) has a length of 22.0 km, while the Santa Monica North Trace (Santa Monica North) has length of 12.8 km (Figure 4).

We consider fault scenarios that involve ruptures extending across the Santa Monica fault, combined with the Anacapa-Dume fault or Malibu Coast fault to the west, and ruptures extending along the Hollywood fault or parallel structure along the Hollywood Basin, and the Raymond fault to the east. In detail, we consider combined ruptures that extend along the Santa Monica North Trace, connecting to the west end of the Hollywood fault, and ruptures that extend along the Santa Monica South Trace and connecting to the eastern reach of the Hollywood fault. The location of these fault segments is shown on Figure 4, and the source parameters (trace length, width of seismogenic zone, fault dip, and slip rate) for each fault are listed in Table 1. The fault segment slip rates listed in Table 1 are minimum, average, and maximum solution slip rates from the UCERF3 “Grand Inversion”, representing the range and average of the slip rates that result from the inversion process (Field et al., 2013; Excel file “ofr2013-1165_FaultSectionData” at <http://pubs.usgs.gov/of/2013/1165/>). These solution rates are based on geologic and geodetic data for the individual faults; and given that the direct information on geologic slip rates for these faults is relatively limited, the constrained range of possible rates resulting from the inversion are considered to be an appropriate representation of fault slip rates for the PFDHA.

Given these fault segments as shown on Figure 4, and that ruptures may extend over one to four fault segments, we developed 18 rupture scenarios that each include rupture along the South Trace or North Trace of the Santa Monica fault (Figure 6a,b,c). Because all of these faults are known to have had latest Pleistocene and/or Holocene rupture, and following the approach of UCERF3, these 18 models all occur at rates that sum to the mean weighted slip rate for all of the faults (representing aleatory variability [defined as randomness in the natural process] of ruptures across the Santa Monica fault). The rupture parameters for each scenario (fault dip, rupture length and width, and slip rate) are based on a rupture-length and a rupture-area weighted average considering all faults that rupture in a given scenario, and are listed in Table 2. Specifically, the rupture width for a fault segment is calculated from the fault dip and thickness of the seismogenic zone, and an average rupture width for each rupture scenario is calculated based on a fault segment length weighted average. The rupture scenario slip rate is then calculated based on a fault-segment rupture area weighted average. Additional notes regarding modifications to the UCERF3 fault segment parameters and geometry are listed on Table 1.

Table 1: Fault Source Parameters from UCERF 3 Models

Fault ¹ (UCERF3 Model)	Trace Length (km)	Fault Dip	Seismogenic width (km)	Rupture Area (km ²)	Slip Rate (mm/yr) ²	Notes on modifications to UCERF 3 parameters
Santa Monica North Trace (FM 3.1 modified)	12.8	75	Top: 0 Bottom: 17.9	239	0.50 1.08 2.13	UCERF 3 trace modified in Century City – Beverly Hills; extends along Santa Monica Blvd, and NE through Los Angeles Country Club to WBHL.
Santa Monica South Trace (FM 3.2 modified)	22	75	Top: 0 Bottom: 17.9	410	0.38 0.79 1.66	UCERF 3 trace modified in Century City – Beverly Hills; extends along Santa Monica Blvd, continues NE across WBHL, Moreno Dr., Wilshire Blvd, and ENE along North Salt Lake fault at south margin of Hollywood Basin. Fault dip and depth taken as for FM 3.1 based on field data.
Hollywood Basin Connecter	9.4	75	Top: 0 Bottom: 17.9	175	0.61 1.29 3.28	Inferred fault trace extending from east end of Hollywood Basin (east end of Santa Monica South Trace) NE and ENE to west end of Raymond fault. Assigned same geometry as Santa Monica South Trace, and slip rate for Hollywood fault.
Hollywood (FM3.1 & FM 3.2)	20.9	70	Top: 0 Bottom: 17.3	350	0.61 1.29 3.28	UCERF 3 trace modified in Beverly Hills to extend 0.1 km westward to Newport-Inglewood North Extension (NINE) and 1.25 km south along NINE to intersection with Santa Monica North Trace
Raymond (FM 3.1 & FM 3.2)	22.5	79	Top: 0 Bottom: 15.6	358	0.51 1.25 2.80	Using UCERF 3 parameters.
Anacapa-Dume (FM 3.2 modified)	66.3	45	Top: 0 Bottom: 11.4	1069	0.33 0.57 2.62	UCERF 3 FM 3.2 trace (64.8 km) extended 1.5 km northeast to intersect west end of Santa Monica Fault (both traces); ruptures assumed to reach surface (Top 0 km).
Malibu Coast (FM 3.2 modified)	36.5	74	Top: 0 Bottom: 16.6	630	0.25 0.76 2.25	UCERF 3 FM 3.2 trace (measured at 38.0 km) truncated 1.5 km west-northwest from east end of trace at intersection of west end of Santa Monica Fault (both traces).
Newport-Inglewood (FM 3.1 modified)	65.7	88	Top: 0 Bottom: 15.0	986	0.77 1.22 1.81	North end of UCERF3 Newport-Inglewood traces is located 1.9 km north-northwest of mapped surface traces of fault. Modeled trace simplified slightly along strike from original UCERF3 trace, and extended south over gap to NIO.
Newport-Inglewood (NI) (FM 3.2)	65.7	90	Top: 0 Bottom: 15.1	993	0.46 0.96 1.79	Used FM3.1 trace as noted above.
Newport-Inglewood North extension (NINE)	5.0	88	Top: 0 Bottom: 15.0	80	0.61 1.09 1.80	Inferred fault trace extending between Newport-Inglewood and Hollywood faults (CGS, 2016). Assigned same geometry as NI FM3.1 fault, and mean of slip rates for both FM3.1 and FM3.2 traces of NI fault

Fault ¹ (UCERF3 Model)	Trace Length (km)	Fault Dip	Seismogenic width (km)	Rupture Area (km ²)	Slip Rate (mm/yr) ²	Notes on modifications to UCERF 3 parameters
West Beverly Hills Lineament	5.3	N/A	N/A	N/A	N/A	Inferred fault trace extending between Newport-Inglewood and Hollywood faults; included in USGS Quaternary fault database. Presumed not active as described in report.
Newport-Inglewood Offshore (NIO) (FM 3.1 & FM 3.2)	66.5	90	Top: 0 Bottom: 10.2	678	0.58 0.99 1.78	Using UCERF 3 parameters.
Rose Canyon (FM3.1 & FM 3.2)	75.2	90	Top: 0 Bottom: 7.7	579	0.88 1.42 1.89	Using UCERF 3 parameters.

Notes:

1. All faults are considered to be strike-slip or oblique strike-slip. Original UCERF 3 fault parameters listed in Excel file ofr2013-1165_FaultSectionData, GeometryData worksheet (<http://pubs.usgs.gov/of/2013/1165/>).
2. Slip rates are UCERF3 Solution minimum, average, and maximum rates for each fault (Excel file ofr2013-1165_FaultSectionData, AveSolSlipRate worksheet (<http://pubs.usgs.gov/of/2013/1165/>), or are taken as noted above.

We also allow for uncertainty in the fault dip, seismogenic width, and rupture length as follows. We assign an uncertainty of ± 10 degrees for fault dip based on judgement and on uncertainty assigned to fault dip in the UCERF studies. We assign an uncertainty in seismogenic depth of -1.2 and +1.1 km based on the uncertainty in depths of well-located earthquakes in the southern California region (Nazareth and Hauksson, 2004), and on judgement from review of plots of seismicity versus depth along faults shown in Nazareth and Hauksson (2004) and from well-located earthquakes along faults selected from earthquake catalogs of southern California.

An additional parameter incorporated in the rupture scenarios is an alternative rupture length for all multi-segment ruptures. The Santa Monica North and Santa Monica South fault segments have lengths of 12.8 and 22 km, respectively, and are considered to represent a minimum rupture length for earthquakes on the Santa Monica fault that are likely to result in surface displacement. The multi-segment ruptures shown in Table 2 have lengths of 31 to 120 km, and to develop a broader distribution of rupture lengths and earthquake magnitudes, we assign an alternate half-length rupture to each multi-segment rupture as an epistemic uncertainty (defined as uncertainty in parameters due to lack of data) for rupture length. The alternate rupture lengths are assigned $\frac{1}{3}$ weight and the total length for each scenario is assigned $\frac{2}{3}$ weight, with higher weight given to the total length because the geomorphic expression along the surface trace of individual fault segments is relatively consistent, supporting the occurrence of ruptures occurring over the entire fault segment. The alternate rupture length are appropriate to consider, however, because recent historical earthquakes worldwide have ruptured across both full and partial fault segments, and because the continuity and expression of the offshore Anacapa-Dume and Malibu Coast faults is not well defined, such that these fault segments are much longer than the segment lengths of the onshore Santa Monica, Hollywood, and Raymond faults (Table 1).

3.2 Scenarios for Rupture of the Newport-Inglewood Fault

Rupture scenarios for the Newport-Inglewood fault are based on models presented by WGCEP (2008), UCERF3 (Field et al., 2013), and additional published and unpublished data. As noted in Section 2.2, two equally weighted alternatives for the location of the Newport-Inglewood fault are presented in WG08 and UCERF3, FM 3.1 and FM 3.2 of UCERF3, respectively. These modeled faults have the same northern endpoint, which is approximately 1.2 miles (1.9 km) north of the northern-most surface exposure of the Newport-Inglewood fault near National Drive in Los Angeles, and about 1.6 miles (2.6 km) south of the WPLE along Wilshire Boulevard (Figure 3).

For the purpose of this evaluation to assess the potential fault displacement hazard associated with a northern extension of the Newport-Inglewood fault, we consider that the Newport-Inglewood fault may extend northwest and north-northwest from the north end of the UCERF3 trace to the south end of the inferred fault trace of CGS (2016), as shown on Figure 3 and Figure 5. The modeled fault extends northwestward along the CGS (2016) fault, through the zone of faulting along Lasky Drive, to intersect the Hollywood fault (Figure 5). This modeled northern extension of the Newport-Inglewood fault is referred to as the Newport-Inglewood North Extension (NINE). The UCERF3 trace of the Newport-Inglewood fault has a total length of about 41 miles (65.7 km), and the NINE extends over 3.1 miles (5 km) to the Hollywood fault. The Newport-Inglewood-NINE rupture scenario thus has a total length of about 44 miles (71 km). For the PFDHA, we allow for alternative rupture lengths of 24 and 44 miles (36 and 71 km), with higher weight ($\frac{2}{3}$) given to the full length rupture following the approach of the WCEP (2008) to allow only full length ruptures on individual fault segments (see Table 3).

Table 2: Source Characteristics for Santa Monica Fault Rupture Scenarios

Fault Scenario ¹	Scenario Length (km)	Rupture Length (km) ²	Dip (degrees) ³	Seismogenic Width (km) ^{3,4}	Slip Rate (mm/yr) ^{3,5}
1. Santa Monica South (SMST)	22	22	65,75,85	16.9, 18.0,19.2	0.38, 0.79, 1.66
2. SMST+HBc	31	31, 16	65,75,85	16.9, 18.0,19.2	0.43, 0.89, 1.99
3. SMST+HBc+RY	54	54, 27	65,75,85	15.9, 17.0,18.2	0.46, 1.04, 2.32
4. AD+SMST	88	88, 45	45,55,65	12.9, 14.0,15.2	0.34, 0.64, 2.33
5. AD+SMST+HBc	98	98, 49	45,55,65	12.9, 14.0,15.2	0.36, 0.68, 2.4
6. AD+SMST+HBc+RY	120	120, 60	50,60,70	12.9, 14.0,15.2	0.39, 0.79, 2.48
7. MC+SMST	58	58, 29	65,75,85	15.9, 17.0,18.2	0.3, 0.77, 2.02
8. MC+SMST+HBc	68	68, 34	65,75,85	15.9, 17.0,18.2	0.33, 0.82, 2.13
9. MC+SMST+HBc+RY	90	90, 45	65,75,85	15.9, 17.0,18.2	0.37, 0.92, 2.29
10. Santa Monica North Trace (SMNT)	13	13	65,75,85	16.9, 18.0,19.2	0.5, 1.08, 2.13
11. SMNT-HY	34	34, 17	65,75,85	15.9, 17.0,18.2	0.56, 1.2, 2.78
12. SMNT-HY-RY	56	56, 28	65,75,85	15.9, 17.0,18.2	0.55, 1.22, 2.79
13. AD+SMNT	79	79, 40	45,55,65	14.9, 16.0,17.2	0.36, 0.68, 2.52
14. AD+SMNT+HY	100	100, 50	45,55,65	14.9, 16.0,17.2	0.42, 0.81, 2.68
15. AD+SMNT+HY+RY	122	122, 61	45,55,65	14.9, 16.0,17.2	0.43, 0.89, 2.7
16. MC+SMNT	49	49, 25	65,75,85	15.9, 17.0,18.2	0.32, 0.85, 2.22
17. MC+SMNT+HY	70	70, 35	65,75,85	15.9, 17.0,18.2	0.4, 0.97, 2.51
18. MC+SMNT+HY+RY	93	93, 46	65,75,85	15.9, 17.0,18.2	0.43, 0.94, 2.12
Notes					
1. Fault segments in scenario listed from west to east. SMN - Santa Monica North Trace; SMST - Santa Monica South Trace; HBc - Hollywood Basin Connector; HY - Hollywood; RY - Raymond; AD - Anacapa Dume; MC - Malibu Coast. See Figures 3 and 6a,b,c for location of faults and fault scenarios, respectively.					
2. The alternate half-length ruptures are assigned 1/3 weight, and the total length ruptures are assigned 2/3 weight.					
3. The three alternative estimates for Fault Dip, Seismogenic Width, and Slip rate are weighted 0.185, 0.63, 0.185.					
4. Seismogenic Width represents bottom depth of rupture, with top of rupture at ground surface.					
5. The three alternative slip rates represent fault area-weighted UCERF3 Solution minimum, average, and maximum rates for fault segments included in rupture scenario.					

For the Newport-Inglewood-NINE scenario rupture, Section 2 of the WPLE extends across the inferred NINE fault at a distance of 1.1 miles (1.8 km) from the north end of the modeled fault (Figure 5). Thus, the WPLE crossing is located close to the end of the fault for this rupture scenario, and the surface displacement is expected to be small compared to the average surface displacement that will occur further south, nearer the middle of the rupture, following the displacement model of Petersen et al. (2011).

Additional scenarios include rupture of the Newport-Inglewood fault southward along the offshore Newport-Inglewood fault and Rose Canyon fault as presented in WGCEP (2008). The combined Newport-Inglewood-NINE – Newport-Inglewood Offshore (NIO) scenario rupture has a total length of 86 miles (139 km); we use alternative rupture lengths of 44 and 86 miles (70 and 139 km), with higher weight ($\frac{2}{3}$) given to the full length rupture following the approach of WGCEP (2008). The combined Newport-Inglewood-NINE – NIO – Rose Canyon (RC) scenario rupture has a total length of 133 miles (213 km); we use alternative rupture lengths of 67 and 133 miles (107 and 213 km), with equal weight given to each rupture length. The parameters for seismogenic width and slip rate for each scenario shown in Table 3 represent a length or area weighted average of the UCERF3 rupture parameters (dip, depth, and slip rate) for the Newport-Inglewood – NINE fault (44 miles [71 km]), NIO fault (42 miles [68 km]), and RC fault (46.5 miles [75 km]). Maps showing the extent of these three rupture scenarios and the WPLE are shown on Figure 7.

We also considered rupture scenarios for combined rupture of the Newport-Inglewood-NINE and the Hollywood fault, or the Santa Monica and offshore faults (Anacapa-Dume and Malibu Coast). Of these possible combined or multi-fault ruptures, we note that the geometry of the intersections of the Santa Monica (both the North Trace and the South Trace) and the Hollywood faults with the NINE may not favor a continuous through-going rupture where the magnitude of displacement would be related to the combined rupture length/area of both faults. Rather, the magnitude of displacement at the crossing of the WPLE likely will be related to the extent of the rupture on either fault, such as described by the scenarios for the Santa Monica fault or the Newport-Inglewood fault. However, because there is considerable uncertainty on the nature of displacements that may occur at the WPLE crossings from this type of multi-fault rupture, we prepared a fault scenario for rupture of the NINE and Hollywood faults (shown on Figure 7) to represent possible scenarios where ruptures may extend along the NINE, crossing the WPLE, and continuing along either of the Santa Monica South Trace or the Hollywood fault. This fault scenario has a total length of 54.7 miles (88 km), and we assign rupture lengths of 28.1 and 54.7 miles (44 and 88 km) as shown in Table 3. The scenario rupture includes the onshore Newport-Inglewood fault, NINE and the Hollywood faults (Figure 5 and Figure 7). Because the displacement on this combined rupture is expected to be strike slip, we assign the same fault dip and fault width as for the Newport-Inglewood fault. The slip rate is the area-weighted average for the three fault segments (Table 3).

We also considered scenarios where rupture on the Newport-Inglewood fault could extend north from the Newport-Inglewood fault on other mapped or inferred faults (i.e., does not extend northward along NINE). In these scenarios, the northern extent of rupture may 1) coincide with the extent of the mapped Quaternary traces near National Blvd, 2) extend north to the possible northern extension of the Newport-Inglewood fault mapped by Treiman et al. (2015), or 3) extend northwest to the Cheviot Hills or to southern part of the WBHL (Figure 3). Because there is no evidence to show that these scenario ruptures extend to the WPLE, they are not assessed for this study.

We did not include a scenario for combined rupture of the Newport-Inglewood and Compton faults because this scenario does not provide a different setting for a potential WPLE crossing of the Newport-Inglewood fault or a different expected magnitude and displacement at the site compared to the rupture scenarios in Table 3. We do not consider scenarios for combined or connected ruptures to occur on the Santa Monica and Newport-Inglewood faults because these scenarios are also not expected to result in a different expected magnitude or displacement at the WPLE compared to scenarios for rupture of the NI, NI – NIO, and NI NINE – Hollywood scenarios. Additional discussion of this issue is provided in Section 4 of this report.

Table 3: Source Characteristics for Newport-Inglewood Fault Rupture Scenarios

Fault Scenario ¹	Scenario Length (km)	Rupture Length (km) ²	Dip (degrees) ³	Seismogenic Width (km) ^{3,4}	Slip Rate (mm/yr) ^{3,5}
1. Newport-Inglewood	66	66, 33	83,88,90	13.9, 15.0,16.2	0.61, 1.09, 1.8
2. Newport-Inglewood-NINE	71	71, 36	83,88,90	13.9, 15.0,16.2	0.61, 1.09, 1.8
3. NI-NINE-NIO	139	139, 70	90.0	11.9, 13.0,14.2	0.6, 1.05, 1.79
4. NI-NINE-NIO-RC	212	212, 107	90.0	9.9, 11.0,12.2	0.67, 1.14, 1.82
5. NI-NINE-Hollywood	88	88, 44	83,88,90	13.9, 15.0,16.2	0.61, 1.14, 2.19
6. NI-NINE-SMST	85	85, 43	83,88,90	13.9, 15.0,16.2	0.54, 1, 1.76
7. NI-NINE-SMST-AD2	150	150, 75	83,88,90	12.9, 14.0,15.2	0.45, 0.81, 2.09

Notes

1. Fault segments in scenario include the Newport-Inglewood (NI), Newport-Inglewood North Extension (NINE), Newport-Inglewood Offshore (NIO), and Hollywood faults. See Figures 3 and 5, and 7 for location of faults and fault scenarios."
2. The alternate half-length ruptures are assigned 1/3 weight, and the total length ruptures are assigned 2/3 weight.
3. The three alternative estimates for Fault Dip, Seismogenic Width, and Slip rate are weighted 0.185, 0.63, 0.185.
4. Seismogenic Width represents bottom depth of rupture, with top of rupture at ground surface.
5. The three alternative slip rates represent area-weighted UCERF3 Solution minimum, average, and maximum rates. For the Newport-Inglewood fault, the slip rate is taken as the mean of the rates for FM3.1 and FM3.2."

4.0 PROBABILISTIC FAULT DISPLACEMENT HAZARD ASSESSMENT

The purpose of this evaluation is to perform a PFDHA to assess the frequency of rupture and amount of displacement that may occur on the postulated northern extension of the Newport-Inglewood fault and the eastern extension of the South Branch of the Santa Monica fault where they pass through the planned alignment of Section 2 of the WPLE.

4.1 Methodology for Probabilistic Fault Displacement Hazard Analysis

The methodology used to evaluate fault displacement hazard is analogous to the well developed formulation for probabilistic evaluation of the hazard due to earthquake strong ground shaking. Logic trees are used to describe the significant input parameters, the uncertainties in the input parameters and their related dependencies. Descriptions and reviews of the methodology for conducting PFDHA are provided by Youngs et al. (2003), Petersen et al. (2011), and American Nuclear Society (2015).

The PFDHA addresses how frequently displacement events occur and how large the displacements are in each event. The hazard can be represented by a displacement hazard curve analogous to ground motion hazard curves. Specifically, the hazard curve is a plot of the annual frequency of events exceeding fault displacement value d , designated by $v(d)$. This frequency is computed by the expression:

$$v(d) = \lambda_{DE} \cdot P(D > d)$$

where λ_{DE} is the frequency at which displacement events occur on the feature (fault) located at the point of interest, and $P(D > d)$ is the conditional probability that the displacement during a single event will exceed value d .

Specific details of the methodology and implementation of the PFDHA are provided in the following sections. Results of the PFDHA are provided in Section 4.2.

4.1.1 Approaches for Frequency of Fault Displacement

Two approaches commonly are used to estimate the frequency of displacement events. The displacement approach provides an estimate based on feature-specific or site-specific estimates of the slip rate, recurrence intervals, and average slip (displacement) per event. The second approach, designated the earthquake approach, involves relating the frequency of slip events at the site to the length, width, and frequency of earthquakes on the fault, and the probability that an individual earthquake will be associated with surface rupture. Due to the lack of specific data regarding average slip per event and recurrence of surface rupturing events for the Santa Monica fault at the point where it crosses the WPLE, the analysis conducted for this study is based only on the earthquake approach.

The earthquake approach methodology for PFDHA, described in Youngs et al. (2003), is parallel to that used for probabilistic seismic hazard assessment (PSHA). Earthquake sources are modeled in terms of their geometry and the frequency of earthquakes of various sizes. The seismic source parameters are used to develop a magnitude-frequency curve for earthquake occurrence on the fault.

4.1.2 Characteristic Earthquakes and Maximum and Average Fault Displacement

Estimates of the expected surface displacements on an individual fault are developed using empirical relationships for estimation of maximum and average surface displacement from earthquake

magnitude. This approach is necessary because no measurements of surface displacement from previous earthquakes that may have ruptured the Santa Monica fault in the Century City – West Beverly Hills area have been identified from observations of fault rupture in paleoseismic investigations (i.e., Dolan et al., 2000; Olson, 2015; Treiman et al., 2015). To use the Earthquake Approach, it is necessary to first assess the expected magnitude for ruptures on the faults. The expected magnitude for rupture on a fault may be evaluated based on a historical large magnitude earthquake occurring on the fault, or in the absence of large magnitude historical earthquakes, typically is assessed from the expected fault rupture length and/or rupture area. In this study, we use equally weighted empirical regression relationships for magnitude from rupture area from Wells and Coppersmith (WC94; 1994) and Hanks and Bakun (02; 2002). Both relationships have been widely used in seismic hazard analyses worldwide; the WC94 relationships are applicable for all slip types, while the HB02 relationship is applicable for strike slip faulting. The HB02 regression is judged to better represent the empirical relationship between magnitude and rupture area for earthquakes larger than about M 7.25, however, so we use both relationships in the analysis.

The frequency distribution of earthquakes of various magnitudes is based on the Youngs and Coppersmith (1985) characteristic earthquake model. We use three weighted alternatives for the b-value in the recurrence relationships, 0.9 (0.185), 0.95 (0.63), 1.0 (0.185); these values were selected based on the analyses of b-values in California presented in Page et al. (2011) and Appendix L of Field et al. (2013).

4.1.3 Probability of Rupture along Alignment

Given the distribution of earthquakes of different sizes, either a magnitude-rupture area or magnitude-rupture length relationship, or both, is then used to characterize the extent of earthquake rupture for each magnitude. For ruptures shorter than the total fault length, each rupture length is distributed uniformly along the fault to assess whether that specific rupture extends along the fault at the closest approach to the site. If a rupture scenario (a specific rupture length at a specific location along the fault) does not rupture along the fault at the closest approach to the site, it is assumed that there is no fault displacement hazard at the site for that specific rupture. The probability of rupture at the site (PRS) for earthquakes of a specific magnitude (and corresponding rupture length) is equal to the number of ruptures that reach the site divided by the total number of ruptures from the uniform distribution of the rupture length along the fault. The probability is summed over each magnitude and corresponding rupture length. Petersen and others (2011) describe this as the rupture location variability.

4.1.4 Probability of Surface Rupture

The PFDHA formulation also includes an assessment of the likelihood of earthquake ruptures reaching the ground surface, expressed as a probability of surface rupture (PSR) versus magnitude. The PSR may be determined from a global assessment of earthquakes that ruptured to the ground surface and earthquakes that did not rupture to the ground surface (Lettis et al., 1997; Petersen et al., 2011). Another approach to assess the PSR is to characterize the rupture width for each magnitude from the corresponding rupture length based on rupture aspect ratios. For this approach, the downdip location of rupture is assigned based on the observed hypocentral depth distribution for the region (LA Basin), and the hypocenter is assigned a uniform distribution over the bottom half of each rupture (Youngs et al., 2003). The PSR at each magnitude is the percentage of ruptures for each rupture width that extend to the surface given the assigned depth distribution for the ruptures. This is referred to as the fault geometry approach for PSR. The fault geometry PSR is sensitive both to the aspect ratio, which may be

on the order of 1:1 for reverse and normal faulting, and 2:1 or larger for strike slip faulting, and the focal depth distribution for the fault assessed from local/regional seismicity. We use the fault geometry approach to assess the probability of surface rupture in this evaluation because we have detailed information on the depth distribution of seismicity for the study area from investigations such as Nazareth and Hauksson (2004) and from well-located events along faults selected from earthquake catalogs for southern California. The PSR is calculated for each rupture width, but typically increases from less than 50% at magnitudes less than about 6.4 to 100% at magnitudes of about 6.9 or larger

The magnitude-frequency distribution is adjusted (multiplied) by the probabilities calculated for the rupture location variability and expected displacement given the distance of the site from the end of the rupture. Because most small- to intermediate-magnitude earthquakes do not rupture to the surface, they do not contribute to the surface fault displacement hazard, while they do contribute to low levels of ground shaking. Thus, fault displacement hazard curves typically reflect the recurrence rate of only the larger magnitude earthquakes a fault may produce.

4.1.5 Probability of Secondary Displacement

In addition to characterizing the amount of displacement that may occur on a fault, a PFDHA also addresses the probability that fault displacement may occur within a specified region adjacent to the fault, given the uncertainty in the precise location of the primary fault(s) and potential secondary fault traces. Potential future fault displacement may occur away from a mapped fault trace for a number of reasons, including variations in accuracy and precision of the fault mapping, complexity of the fault traces, natural variations in the patterns of surface fault rupture, and occurrence of secondary displacement on faults located near the primary fault trace (Petersen et al., 2011).

The potential for principal faulting diminishes with distance from the mapped fault trace, and the rate of decrease depends on the location confidence of the mapping (i.e., well-located, approximately-located, inferred, or buried) and complexity of the fault trace. The potential for secondary, off-fault displacement also decreases with distance from the mapped fault trace; however, this decrease is significantly more gradual than for principal faulting (Petersen et al., 2011). A recent study of the surface deformation resulting from the 1992 Landers, California earthquake based on detailed comparisons of pre- and post-earthquake aerial photographs shows that the amount of distributed secondary deformation (as a percentage of the displacement on the primary fault) varied significantly along the fault and increased with increasing fault complexity and at the southern end of the rupture (Milliner et al., 2015). Importantly, this study shows that the deformation tended to be distributed across a broader zone rather than localized on one or more discrete fault traces where the fault was structurally complex.

4.1.6 Selection of Primary versus Secondary Fault Displacement Models

The planned alignment of the WPLE crosses the mapped location of the Santa Monica fault at a high angle. Therefore, it is assumed that primary fault displacement may occur at the subway crossing. Therefore, in this study, we calculated the potential for primary fault displacement as an initial assessment of the expected displacement at subway alignment. In addition, because the available data regarding the possible location of faulting do not clearly define the location of primary faulting versus secondary faulting, for this assessment, we assume that primary displacement may occur anywhere with the area that the faults are constrained to underlie. If new information from ongoing investigations provides additional constraints regarding the location of primary versus secondary faulting, additional

assessments of the expected secondary deformation may be performed to further describe the expected deformation across the fault zones.

4.1.7 Fault Displacement Models

The ground motion attenuation relationships used in PSHA are replaced by relationships between earthquake size and the amount of fault offset that may be produced at a point on a fault at (or near) the ground surface. These relationships incorporate the statistical variability in displacements observed in past earthquakes and the variability in fault offset along the length of an earthquake rupture. The fault displacement relationships presented by Youngs et al. (2003) were developed from analysis of normal fault ruptures. More recent studies by Peterson et al. (2011) and Moss and Ross (2011) provide relationships for the variability of displacements along strike-slip and reverse ruptures, respectively. In general, observed and modeled slip distributions peak in middle portions of the rupture, and fall off toward the end of the rupture. In most published methods, the site distance from the end of the rupture is normalized to the rupture length (x/L or l/L) based on the assumption that the site location is equally likely to be on either side of the mid-point of the rupture. Parameter L is the rupture length, and x or l is the distance of the site to the closest end of the rupture. A schematic representation of the geometry of a rupture on a fault and the descriptor variables for PFDHA is shown on Figure 8(A). Typically, slip distributions are also provided in normalized form (e.g. D/D_{max} or D/D_{ave}) for each x/L or l/L , and estimates of D_{max} or D_{ave} can be applied for the magnitude of interest, where D is displacement (maximum or average). At each x/L value, a distribution about the median D/D_{max} or D/D_{ave} estimate is also provided. The distributions vary depending on the model fit to the data. Distributions such as lognormal, Gamma, Beta and Weibull have been applied to model slip distributions (Youngs et al., 2003; Petersen et al., 2011; and Moss and Ross, 2011). Comparison of the different displacement regression models (bilinear, quadratic, elliptical) in Petersen et al. (2011) show that the displacement results are slightly sensitive to the displacement model (D or D/D_{ave}), but are less sensitive to the form of the regression. A plot of the bi-linear regression model for normalized displacement [$\ln(D/D_{ave})$] versus the on-fault distance ratio (l/L) is shown on Figure 8(B).

As described in Section 3, slip on the Santa Monica and Newport-Inglewood faults is assessed as strike slip or strike slip-reverse. Because the dominant expected slip type for future ruptures is strike-slip, we assessed the calculated results for variability in fault displacement considering the strike-slip relationship of Petersen et al. (2011). Thus, for the analysis conducted in this study, probabilistic relationships between earthquake magnitude and fault displacement at a point were constructed using the Wells and Coppersmith (1994) lognormal distributions for average fault offset for all-slip-type earthquakes (to represent D_{ave} for strike-slip faulting), combined with the statistical relationships for variability of displacement along the rupture for strike-slip ruptures. For strike-slip faulting, we use a normalized displacement model (D/D_{ave}) with the bi-linear regression form of Petersen et al. (2011; Figure 8(B)) as the authors expressed no specific preference for any of the displacement models they tested, and because the difference in results among the different displacement models is relatively small.

4.2 Results of the PFDHA –Santa Monica Fault

The results of the PFDHA are presented as fault displacement hazard curves that relate the amplitude of fault offset to the frequency at which it is exceeded. The displacement hazard for the Santa Monica fault individual rupture scenarios is presented in Section 4.2.1. The approach and weighting scheme for developing a weighted mean result for the 18 rupture scenarios is presented in Section 4.2.2, and a

summary of the mean result and the Metro Design Criteria are presented in Section 4.2.3. A summary of return periods for the calculated displacements for each fault is presented in Section 4.2.4

4.2.1 Displacement Hazard for the Santa Monica Fault Rupture Scenarios

The full PFDHA for the Santa Monica fault results represent a probabilistic assessment for the source parameters of rupture length, rupture location along the fault, slip type, slip rate, and PSR. These parameters are considered in the rupture scenarios for the Santa Monica fault, where these 18 scenarios represent aleatory variability in the extent of ruptures that extend along the Santa Monica and adjoining faults. Epistemic uncertainty is considered through alternative values for scenario rupture length, dip, depth, and slip rate as shown in Table 2 and Table 4.

The displacement hazard from the PFDHA is calculated as the annual frequency of exceedance for displacement, where the hazard is initially calculated for each scenario, and the scenarios are then weighted to calculate a mean displacement hazard for all 18 scenarios. Mean hazard is the basic result of both probabilistic seismic hazard and probabilistic fault displacement hazard analyses, and represents the expected annual frequency of exceeding of various levels of ground motion or displacement, respectively. Displacements that have an expected frequency of exceedance corresponding to selected return periods, including a 4 percent probability of exceedance (PE) in 100 years and a 50 percent PE in 100 years, are calculated from the displacement hazard results. The 4 percent and 50 percent PE in 100 years are approximately equivalent to a 2,450-year return period and 144-year return period, respectively, and as noted in Section 1.1, these displacement exceedance return periods correspond to the Maximum Design Earthquake (MDE) and Operating Design Earthquake (ODE) ground shaking exceedance levels. Displacements for other expected annual frequencies of exceedance can be obtained directly from the total hazard curve on Figure 9.

The displacement hazard shows a wide range of results, in particular, representing the sensitivity of the displacement hazard to the site location within earthquake ruptures and the rupture length/area of the individual scenarios. A summary of the x/L value for the total fault length, the mean magnitude for all weighted rupture combinations, and the assigned weight for each of the 18 rupture scenarios is shown in Table 4. The hazard results for the 18 scenarios are combined as described in the following section to develop a mean displacement exceedance estimate for the Section 2 fault crossing.

The x/L values, which range from 0 for a site at the end of a rupture to 0.5 for a site located in the middle $\frac{2}{3}$ of rupture, provide a measure of how close the site lies to the end of a rupture scenario (Figures 6a,b,c). The scenarios that have low x/L values all result in small or no displacement exceedance for a 2,450 year RP, and typically, the scenarios that have high x/L values result in displacement exceedance of 4 inches (10 cm) or more for a 2,450 year RP, with the exception of scenarios that include the Anacapa-Dume fault (Table 4). Because of the longer length of the scenarios that include the Anacapa-Dume fault, the expected magnitude is large (7.3 and larger), and given the low slip rates, the average return period for these large earthquakes is longer than 2,500 years. Therefore, these longer ruptures/larger magnitude earthquakes are not expected to result in a significant displacement exceedance hazard at a 2,450 year RP when considered as an individual earthquake scenario, but they do contribute to the mean hazard for all scenarios.

As noted above, the displacement exceedance hazard at 2,450 years typically is lower for the scenarios that include three or four segments because the recurrence rate for larger ruptures with higher characteristic magnitudes is lower than for the recurrence rate for single or two fault segment rupture

scenarios, and the decrease in recurrence rate has a larger effect on the displacement exceedance hazard than the increase in average displacement that results from the higher magnitude of these earthquake. Therefore, even though the scenarios with longer ruptures result in larger surface displacements, these ruptures occur less frequently, and result in lower displacement exceedance hazard.

Table 4: Santa Monica Fault rupture Scenario Parameters and Weights

Fault Scenario ¹	Scenario Length (km)	X/L Value for Total Length ²	Mean Magnitude ³	Scenario Weight ⁴
1. Santa Monica South (SMST)	22	0.48	6.7	0.053
2. SMST+HBc	31	0.37	6.8	0.212
3. SMST+HBc+RY	54	0.21	7.0	0.111
4. AD+SMST	88	0.12	7.3	0.078
5. AD+SMST+HBc	98	0.20	7.4	0.062
6. AD+SMST+HBc+RY	120	0.35	7.4	0.044
7. MC+SMST	58	0.18	7.0	0.081
8. MC+SMST+HBc	68	0.29	7.1	0.065
9. MC+SMST+HBc+RY	90	0.47	7.3	0.045
10. Santa Monica North Trace (SMNT)	13	0.09	6.5	0.004
11. SMNT-HY	34	0.35	6.8	0.071
12. SMNT-HY-RY	56	0.21	7.0	0.049
13. AD+SMNT	79	0.01	7.2	0.026
14. AD+SMNT+HY	100	0.22	7.4	0.021
15. AD+SMNT+HY+RY	122	0.36	7.5	0.015
16. MC+SMNT	49	0.02	7.0	0.027
17. MC+SMNT+HY	70	0.31	7.1	0.022
18. MC+SMNT+HY+RY	93	0.48	7.3	0.015

Notes

1. Fault segments listed from west to east. SMNT - Santa Monica North; SMST - Santa Monica South; HBc - Hollywood Basin Connector; HY - Hollywood; RY - Raymond; AD - Anacapa Dume; MC - Malibu Coast. See Figures 3 and 6a,b,c for location of faults and fault scenarios, respectively."
2. X/L represents the ratio of the distance of the site from the closest end of the rupture (X) to half the total rupture length (L)
3. Represents mean magnitude for weighted rupture length and rupture width combinations for each rupture scenario.
4. Weights represented normalized product of probabilities for rupture continuity between faults, partitioning of ruptures among alternative Malibu Coast and Anacapa Dume fault, partitioning of displacement between Santa Monica North Trace and Santa Monica South Trace, and probability of single segment rupture."

4.2.2 Mean Displacement Hazard for the Santa Monica Fault

The rupture scenarios selected for this study represent a range of potential ruptures that may result in displacement at fault crossings along Section 2 of the WPLE. These scenarios and displacement estimates must be combined in a probabilistic framework as part of the PFDHA process to calculate the mean displacement hazard. We developed a framework that considers factors of the relative frequency

or portioning of ruptures on alternative faults, the probability that an earthquake rupture will cross between adjacent faults, the distribution of displacement across traces of the Santa Monica fault, and the probability that single segment fault ruptures on the Santa Monica fault represent the maximum rupture.

The probability that ruptures continue from the Santa Monica to adjacent faults (Malibu Coast, Anacapa Dume, Hollywood, Hollywood Basin Connector, and to the Raymond fault adjoining the Hollywood and Hollywood Basin Connector faults) was assessed based on the known timing of past ruptures on each fault and the geometry of the fault connections. The fault combinations and assigned probabilities that any rupture extends between the faults is as follows:

Fault Combination	Probability of Rupture Continuity Between Faults
Anacapa-Dume and Santa Monica (both traces)	0.6
Malibu Coast and Santa Monica (both traces)	0.6
Santa Monica South and Hollywood Basin Connector	0.8
Hollywood Basin Connector and Raymond	0.7
Santa Monica North and Hollywood	0.8
Hollywood and Raymond	0.7

For ruptures with more than two fault segments, the probabilities are multiplied. The probabilities for ruptures to cross to the offshore Anacapa-Dume and Malibu Coast faults is assessed to be slightly lower than for ruptures to cross among the onshore Santa Monica, Hollywood, Hollywood Basin Connector, and Raymond faults because the nature of the connection of the Santa Monica and faults offshore to the west is poorly known compared to the onshore fault connections east from the Santa Monica fault.

The Anacapa-Dume and Malibu Coast faults represent alternative faults that may rupture with the Santa Monica fault. To partition ruptures between them, we assign a relative weight that each fault ruptures with the Santa Monica fault based on the ratio of the weighted average slip rate for the Anacapa-Dume and Malibu Coast faults:

Fault	Slip Rate (Min, Ave, Max, weighted at 0.185, 0.63, 0.185)	Percentage of Ruptures
Anacapa Dume	0.33, 0.57, 2.62.	0.49
Malibu Coast	0.25, 0.79, 2.19	0.51

The Santa Monica South Trace-Hollywood Basin (SMST) and the Santa Monica North Trace (SMNT) both represent potential locations for ruptures on the Santa Monica fault. Because both faults appear to be active, and because the traces are close to each other, it is possible that both faults may rupture during large earthquakes, and that displacement may be distributed along both faults. Given that both faults

may rupture in some or all large earthquakes, it is reasonable to partition displacements from each rupture among the two traces of the Santa Monica fault.

To partition displacements between the SMST and SMNT traces, we considered two options: 1) the ratio of the UCERF3 slip rates (Table 1), and 2) field evidence from Century City and Beverly Hills for the relative activity of each fault. We judged that the field evidence for activity is a more appropriate basis for partitioning ruptures between the SMNT and SMST fault segments, because the available slip rate data is not based on geologic data from the Century City and Beverly Hills area. The presence of the distinct graben(s) along the SMST in the Century City and Beverly Hills area as described in Section 2 provides clear evidence for multiple latest Pleistocene and Holocene ruptures, and indicates that substantial displacement has been accommodated along the SMST. On this basis, most displacement is assumed to occur along the SMST, with a subordinate displacement occurring along the SMNT.

Fault	Evidence for latest Pleistocene-Holocene Activity	Percentage of Displacement
SMNT	Uncertain	0.25
SMST	Strong	0.75

We implemented the distribution of slip in the PFDHA by assuming that all earthquakes may rupture both traces of the Santa Monica fault, and that on the average, 75 percent of the rupture displacement during each postulated event occurs along the Santa Monica South Trace. Therefore, in this assessment, all ruptures on either the South or North Traces may cause displacement at the Section 2 crossings of the Santa Monica South Trace. To evaluate the expected displacement at the WPLE crossings, we modify the empirical relationship used in the PFDHA to calculate average displacement from magnitude to produce 75 percent of the displacement that would be calculated from the original relationship of Wells and Coppersmith (1994). The remaining 25 percent of expected displacement is assumed to occur away from the SMST and the fault crossings for the WPLE, such as along the SMNT.

For potential single segment ruptures of SMNT and SMST, we also assign a probability that this single segment rupture may occur as the characteristic earthquake: These probabilities are low because the mean characteristic earthquake for these segments is in the range of M 6.5 to 6.7, and earthquakes of this magnitude appear too small to generate the distinct geomorphic expression and other structural features identified along the Santa Monica fault.

Fault Segment	Rupture Length (km)	Probability for Single Segment Rupture
SMNT	12.8	0.05
SMST	22.0	0.2

The products of the cumulative probabilities for rupture continuity, distribution of ruptures among the Anacapa-Dume and Malibu Coast faults, distribution of displacement on SMNT and SMST faults for each

rupture scenario were normalized to develop a weight for each scenario as shown in the right-most column of Table 4. The resulting weights range from 0.004 to 0.212. The hazard results for individual fault rupture scenarios are multiplied by the normalized weights and summed to develop a weighted mean hazard curve as shown on Figure 9; the weighted individual hazard curves also are shown on Figure 9. The displacement with a mean frequency of exceedance corresponding to specified returns periods are shown in Table 5 below.

Table 5: Mean Displacement Hazard for Santa Monica Fault

Fault Rupture Scenario	Displacement Model	Return Period (years)	Expected Displacement Exceedance (cm)
Santa Monica Fault – Weighted Mean Result	Full PFDHA	150 (ODE)	<1
		2,450 (MDE)	13.0

The displacement exceedance for the MDE is relatively small, about 5.1 inches (13 cm) because the expected return period for large magnitude earthquakes to occur on the Santa Monica fault is longer than about 2,500 years. However, the displacement hazard curve is relatively flat at the exceedance frequency corresponding to the MDE, such that the displacement exceedance noted above is relatively sensitive to increases or decreases in the calculated hazard level. We performed additional analyses to assess the sensitivity of the displacement hazard to several of the input parameters used in the PFDHA. Considering possible changes to the input parameters for rupture length and fault slip rate, we note that an increase in slip rate increases the displacement hazard for the MDE, while increasing rupture length and magnitude results in a decrease in displacement hazard for the MDE (longer rupture lengths correspond to larger magnitude, less frequent earthquakes).

4.2.3 Return Periods for Santa Monica Fault Displacement Exceedance

As an additional representation of the displacement hazard, we calculate the return period for displacements equal to or exceeding displacements of engineering interest for the Santa Monica Fault in Table 6 below.

Table 6: Expected Return Periods for Displacement Exceedance – Santa Monica Fault

Displacement (cm)	Return Period for Displacement Exceedance (years)
1	1,910
5	2,100
10	2,320
50	4,080
100	6,500
200	12,100

4.3 Results of the PFDHA –Newport-Inglewood Fault

The displacement hazard for the Newport-Inglewood fault rupture scenarios is presented in Section 4.3.1. The approach and weighting scheme for developing a weighted mean result for the seven rupture

scenarios is presented in Section 4.3.2, and a summary of the mean result and the Metro Design Criteria are presented in Section 4.3.3. A summary of return periods for the calculated displacements for each fault is presented in Section 4.3.4.

4.3.1 Displacement Hazard for the Newport-Inglewood Fault Rupture Scenarios

The full PFDHA for the Newport-Inglewood fault results represent a probabilistic assessment for the source parameters of rupture length, rupture location along the fault, slip type, slip rate, and PSR. These parameters are considered in the rupture scenarios for the Newport-Inglewood fault, where the selected scenarios represent aleatoric variability in the extent of ruptures along the Newport-Inglewood and adjoining faults. Epistemic uncertainty is considered through alternative values for scenario rupture length, dip, depth, and slip rate as shown in Table 3 and Table 7.

The displacement hazard from the PFDHA is calculated as the annual frequency of exceedance for displacement, where the hazard is initially calculated for each scenario, and the scenarios are weighted to calculate a mean displacement hazard for the selected rupture scenarios. As for the Santa Monica fault, displacements that have an expected frequency of exceedance corresponding to 4 percent probability of exceedance (PE) in 100 years, and 50 percent PE in 100 years, are calculated from the displacement hazard results

The displacement hazard shows a wide range of results, in particular, representing the sensitivity of the displacement hazard to the site location within earthquake ruptures and the rupture length/area of the individual scenarios. A summary of the x/L value for the total fault length, the mean magnitude for all weighted rupture combinations, and the assigned weight for each of the rupture scenarios is shown in Table 7. The hazard results for four selected scenarios are combined as described in the following section to develop a mean displacement exceedance estimate for the Section 2 fault crossing.

For the scenarios that involve only the north-northwest trending fault segments, Rose Canyon-Newport-Inglewood Offshore, Newport-Inglewood, and NINE (Scenarios 1 to 4 on Figure 7), the site is always located near the end of a rupture, resulting in low x/L values (0.01 to 0.03; Table 7). Thus, the expected displacements for these scenario ruptures will always be small. Further, because the range of slip rates for the scenario ruptures is low (0.6 to 1.8 mm/yr; Table 3), mm/yr, the expected return period for scenario ruptures typically is several thousand years or longer.

Because of the longer length of the scenarios that include the Newport-Inglewood Offshore and Rose Canyon faults, the expected magnitude is larger (7.3 and larger), and given the low slip rates, the average return period for these large earthquakes is much longer than 2,500 years. Therefore, these longer ruptures/larger magnitude earthquakes are not expected to result in a significant contribution to displacement exceedance hazard at a 2,450 year RP.

4.3.2 Mean Displacement Hazard for the Newport-Inglewood Fault

The rupture scenarios selected for this study represent a range of potential ruptures that may result in displacement at the Lasky Drive fault crossing along Section 2 of the WPLE. To assess the relative frequency of the scenario ruptures, we considered the participation plots from UCERF3 (Field et al, 2013) that show how frequently adjoining or connected faults rupture along with the Newport-Inglewood fault. As described in Section 2.2, these plots show that the Newport-Inglewood Offshore and Rose Canyon faults rupture much more frequently with the Newport-Inglewood fault than do faults to

the north. Therefore, we assign relatively high weight to the Newport-Inglewood-NINE (0.40), and Newport-Inglewood Offshore-Newport Inglewood –NINE scenarios (0.30), and low weight to the longer scenario that also includes the Rose Canyon faults (NINE-NI-NIO; 0.10) because there is no strong evidence to show that the entire fault system may rupture in a single event. Although we do not think ruptures are likely to extend northward from the NINE to the Santa Monica or Hollywood faults, we assign some weight to the Newport-Inglewood-NINE-Hollywood scenario (0.2) as it represents one of several potential ruptures for which the x/L values would be much larger than for the ruptures occurring only along the Rose Canyon to NINE faults (Table 7).

Table 7: Newport-Inglewood Fault Rupture Scenario Parameters and Weights

Fault Scenario ¹	Scenario Length (km)	X/L Value for Total Length ²	Mean Magnitude ³	Scenario Weight ⁴
1. Newport-Inglewood	66	0.00	7.0	0.00
2. Newport-Inglewood-NINE	71	0.03	7.1	0.40
3. NI-NINE-NIO	139	0.01	7.3	0.30
4. NI-NINE-NIO-RC	212	0.01	7.4	0.10
5. NI-NINE-Hollywood	88	0.21	7.2	0.20
6. NI-NINE-SMST	85	0.15	7.2	0.00
7. NI-NINE-SMST-AD2	150	0.46	7.3	0.00

Notes

1. Fault segments in scenarios include the Newport-Inglewood (NI), Newport-Inglewood North Extension (NINE), Newport-Inglewood Offshore (NIO), Rose Canyon, Hollywood, Santa Monica, and Anacapa Dume faults. See Figures 3, 5, and 7 for location of faults and fault scenarios."
2. X/L represents the ratio of the distance of the site from the closest end of the rupture (X) to half the total rupture length (L).
3. Represents mean magnitude for weighted rupture length and rupture width combinations for each rupture scenario.
4. Weights represent subjective assessment of the relative frequency of rupture scenarios. Scenario no. 1 for the Newport-Inglewood fault is assigned zero weight; this rupture would not reach the site, therefore, assigning weight to this scenario would decrease the displacement hazard for the WPLE. Scenarios nos. 6 and 7 both could represent a rupture at the WPLE, but are assigned zero weight because the potential rupture hazard is reasonably represented by other scenarios for the Newport-Inglewood and Santa Monica faults. See text of report for further discussion.

The hazard results for the four individual fault rupture scenarios are multiplied by the weights and summed to develop a weighted mean hazard curve as shown on Figure 10; the weighted individual hazard curves also are shown this figure The displacement with a mean frequency of exceedance corresponding to specified returns periods are shown in Table 8 below.

Table 8: Mean Displacement Hazard for Newport-Inglewood Fault

Fault Rupture Scenario	Displacement Model	Return Period (years)	Expected Displacement Exceedance (cm)
Newport-Inglewood Fault – Weighted Mean Result	Full PFDHA	150 (ODE)	<1
		2,450 (MDE)	<1

As shown on Figure 10, and in Table 8, the displacement hazard for the Lasky Drive crossing of the Newport-Inglewood fault is negligible. While, as noted for the Santa Monica fault, the displacement hazard is particularly sensitive to changes in fault slip rate, the hazard for the Newport-Inglewood fault

is low, such that potential changes in the fault slip rate would not result in a significant change in the displacement hazard for the MDE.

4.3.3 Return Periods for Newport-Inglewood Fault Displacement Exceedance

As an additional representation of the displacement hazard, we calculate the return period for displacements equal to or exceeding displacements of engineering interest for the Newport-Inglewood Fault in Table 9 below.

Table 9: Expected Return Periods for Displacement Exceedance – Newport -Inglewood Fault

Displacement (cm)	Return Period for Displacement Exceedance (years)
1	4,780
5	5,350
10	6,070
50	11,200
100	17,500
200	31,200

4.4 Summary of Fault Displacement Parameters

The purpose of this evaluation is to develop probabilistic estimates of fault displacement at the WPLE for two performance levels, the Operating Design Earthquake (ODE) and Maximum Design earthquake (MDE). These probabilistic displacement estimates are provided for use in design of Section 2 of the WPLE.

It is expected additional investigations will provide specific information on location and nature of the fault crossings, but for the purpose of this evaluation, we conclude the following:

Santa Monica Fault

- The estimated displacement for the ODE is less than 0.5 inch (<1 cm);
- The estimated displacement for the MDE is 5.1 inches (13.0 cm); and
- Based on the above results and sensitivity analyses, the fault displacement values for the tunnel may be taken as up to 1 centimeter (cm) for the same annual probability of exceedance as defined for ground shaking at the ODE level, and 13 cm for the same annual probability of exceedance as defined for ground shaking at the MDE level.

Newport-Inglewood Fault

- The estimated displacement for the ODE is less than 0.5 inch (<1 cm);
- The estimated displacement for the MDE is less than 0.5 inch (<1 cm); and

- Based on the above results and sensitivity analyses, the fault displacement values for the tunnel for the Newport-Inglewood fault may be taken as up to 1 centimeter (cm) for the same annual probability of exceedance as defined for ground shaking at both the ODE level and MDE level.

5.0 LIMITATIONS

In the performance of our professional services, Amec Foster Wheeler, its employees, and its agents comply with the standards of care and skill ordinarily exercised by members of our profession practicing in the same or similar localities. No other warranty, either express or implied, is made or intended in connection with the work performed by us, or by the proposal for consulting or other services, or by the furnishing of oral or written reports or findings. We are responsible for the conclusions and recommendations contained in this report, which are based on data related only to the specific project and locations discussed herein. In the event conclusions or recommendations based on these data are made by others, such conclusions and recommendations are not our responsibility unless we have been given an opportunity to review and concur with such conclusions or recommendations in writing.

6.0 REFERENCES

- American Nuclear Society, 2015, Criteria for Assessing Tectonic Surface Fault Rupture and Deformation at Nuclear Facilities: American National Standard ANSI/ANS-2.30-2015, 50 p.
- Bryant, W.A., 1988, Recently active traces of the Newport-Inglewood fault zone, Los Angeles and Orange counties, California: California Division of Mines and Geology Open-File Report 88-14
- Bryant, W.A., (compiler), 2005, Digital Database of Quaternary and Younger Faults from the Fault Activity Map of California, Version 2.0, California Geological Survey Web Page, http://www.conrv.ca.gov/CGS/information/publications/QuaternaryFaults_ver2.htm 8-13-07.
- California Geological Survey (CGS), 1986, Alquist-Priolo Special Studies Zone Map, Inglewood Quadrangle (Revised Official Map): scale 1:24,000, Sacramento, California.
- California Geological Survey, 2016, Preliminary Geologic Map of the Los Angeles 30' x 60' Quadrangle, California, scale 1:100,000.
- Campbell, R.H., Wills, C.J., Irvine, P.J., and Swanson, B.J., 2014, Preliminary geologic map of the Los Angeles 30' x 60' quadrangle, California: Version 2.1: California Geological Survey, Preliminary Geologic Maps, scale 1:100,000, updated 2016.
- Dolan, J.F and Pratt, T.L., 1997, High-Resolution Seismic Reflection Profiling Of the Santa Monica Fault Zone, West Los Angeles, California, Geophysical Research Letters, Vol. 24, No. 16, pp. 2051-2054.
- Dolan, J.F. and Sieh, K., 1992, Tectonic Geomorphology of the Northern Los Angeles Basin: Seismic Hazards and Kinematics of Young Fault Movement, in Ehlig, P.L., and Steiner, E.A., eds., Engineering Geology Field Trips: Orange County, Santa Monica Mountains, and Malibu, Guidebook and Volume: Berkley, California, Association of Engineering Geologists, p. B20-26.
- Dolan, J.F., Sieh, K., Rockwell, T.K. Yeats, R.S., Shaw J., Suppe, J., Huftile, G., and Gath, E., 1995, Prospects for Larger or More Frequent Earthquakes in the Los Angeles Metropolitan Region, California, Science, Vol. 267, pp. 199-205.
- Dolan, J.F., Sieh, K.E., Rockwell, T.K., Guptil, P., and Miller, G., 1997, Active Tectonics, Paleoseismology, and Seismic Hazards of the Hollywood Fault, Northern Los Angeles Basin, California, Geological Society of America Bulletin, Vol. 109, No. 12.
- Dolan, J.F., Sieh, K., and Rockwell, T.K., 2000, Late Quaternary Activity and Seismic Potential of the Santa Monica Fault System, Los Angeles, California, Geological Society of America Bulletin, Vol. 112, No. 10.
- Field, E.H., Biasi, G.P., Bird, P., Dawson, T.E., Felzer, K.R., Jackson, D.D., Johnson, K.M., Jordan, T.H., Madden, C., Michael, A.J., Milner, K.R., Page, M.T., Parsons, T., Powers, P.M., Shaw, B.E., Thatcher, W.R., Weldon, R.J., II, and Zeng, Y., 2013, Uniform California earthquake rupture forecast, version 3 (UCERF3)—The time-independent model: U.S. Geological Survey Open-File Report 2013–1165, 97 p., California Geological Survey Special Report 228, and Southern California Earthquake Center Publication 1792, <http://pubs.usgs.gov/of/2013/1165/>.

- Geocon West, Inc., 2013; Fault Rupture Hazard Investigation, 1801 Avenue of the Stars, 10250 Santa Monica Boulevard, 1930 Century Park West, Century City, Los Angeles, California: report prepared for Westfield, Los Angeles, California, 289 p., October 18.
- Geocon West, Inc., 2014; Phase II Site-Specific Fault Rupture Investigation, 9900 Wilshire Boulevard, Beverly Hills, California: report prepared for Allen Matkins Leck Gamble Malory & Natsis LLP, Los Angeles, California, 325 p., May 6.
- Hanks, T.C., and Bakun, W.H., 2002, A bilinear source-scaling model for M–log A observations of continental earthquakes: *Bulletin of the Seismological Society of America*, v. 92, p. 1841–1846.
- Hanks, T.C., and Bakun, W.H., 2014, M-log A models and other curiosities: *Bulletin of the Seismological Society of America*, v. 104, no. 5, p. 2604-2610
- Hanks, T.C., and Kanamori, H., 1979, A moment magnitude scale: *Journal of Geophysical Research*, v. 84, B5, p. 2348-2850.
- Hauksson, E., and Gross, S, 1991, Source parameters of the 1933 Long Beach earthquake: *Bulletin of the Seismological Society of America*, v. 81, p. 81–98.
- Hecker S., Abrahamson, N.A., and Wooddell, K.E., 2013, Variability of Displacement at a Point: Implications for Earthquake-Size Distribution and Rupture Hazard on Faults: *Bulletin of the Seismological Society of America*, v. 103, no.2A, p. 651–674.
- Hildenbrand, T.G., Davidson, J.G., Ponti, D.J., and Langenheim, V.E., 2001, Implications for the Formation of the Hollywood Basin from Gravity Interpretations of the Northern Los Angeles Basin, California: U.S. Geological Survey Open-File Report 2001-394
- Hill, R.L., Slade, R.C., Sprott, E.C., and Bennett, J.H., 1979, Fault location and fault activity assessment by analysis of historic leveling data, oil well data, and ground water data, Beverly Hills-Hollywood area, California: in *Geologic Guide and Engineering Geology Case Histories*, Los Angeles Metropolitan Area, California, Association of Engineering Geologists, First Annual California Section Conference, May12-14, 1978, p. 167-174.
- Hummon, C., Schneider, C.L., Yeats, R.S., and Huftile, G.J., 1992, Active Tectonics of the Northern Los Angeles Basin: An Analysis of Subsurface Data, in *Proceedings of the 35th Annual Meeting of the Association of Engineering Geologists*.
- Hummon, C., Schneider, C.L., Yeats, R.S., Dolan, J.F., Sieh, K.E. and Huftile, G.J., 1994. Wilshire fault: Earthquakes in Hollywood?. *Geology*, v. 22, no. 4, p.291-294.
- Kenny Geoscience, 2014, Structural and stratigraphic evaluation of the Century City - Cheviot Hills area, California: report prepared for Beverly Hills Unified School District, Beverly Hills, California, July.
- Jennings, C.W., and Bryant, W.A., 2010, Fault Activity Map of California: California Geological Survey Geologic Data Map No. 6, scale 1:750,000.

- Leighton Consulting, Inc., 2012, Second Response to California Geological Survey Review Comments, Fault Rupture Hazard Evaluation, Beverly Hills High School, 241 South Moreno Drive, Beverly Hills, California, CGS Application No. 03-CGS0960, 446 p., December 28.
- Leighton Consulting, Inc., 2015, Geohazard Report, El Rodeo K-8 School, 605 Whittier Drive, Beverly Hills, Los Angeles County, California: report prepared for Beverly Hills Unified School District, Beverly Hills, California, 186 p., March 2.
- Leighton Consulting, Inc., 2016, Updated Fault Hazard Assessment and Response to CGS Review Letter, El Rodeo K-8 School, 655 Whittier Drive, Beverly Hills, California: report prepared for Beverly Hills Unified School District, Beverly Hills, California, 445 p., January 31, 2016.
- Lettis, W.R., Wells, D.L., and Baldwin, J.N., 1997, Empirical Observations Regarding Reverse Earthquakes, Blind Thrust Faults, and Quaternary Deformation: Are Blind Thrust Faults Truly Blind?" *Bulletin of the Seismological Society of America*, v. 87, no. 5, pp. 1171–1198.
- Los Angeles County Metropolitan Transportation Authority (Metro), 2011, Westside Subway Extension Century City Area Fault Investigation Report; report prepared by Parson Brinkerhoff and AMEC, two volumes, November.
- Metro, 2016a, Fault Investigation Report Transects 5 & 6-Tunnel Reach 6, Westside Purple Line Extension Project, Section 3, dated October 11, 2016.
- Metro, 2016b, Section 2 Geotechnical Fault Investigations Summary Memorandum, dated November 2016.
- Metro, 2017, Fault Investigation Report Tract 9-Tunnel Reach 5, Westside Purple Line Extension Project, Section 2, dated February 2, 2017.
- Milliner, C.W.D., Dolan, J.F., Hollingsworth, J., Leprince, S., Ayoub, F., and Sammis, C.G., 2015, Quantifying near-field and off-fault deformation patterns of the 1992 Mw 7.3 Landers earthquake: Geochemistry, Geophysics, Geosystems, v. 16, doi:10.1002/2014GC005693.
- Moss, R.E.S., and Ross, Z.E., 2011, Probabilistic fault displacement analysis for reverse faults: *Bulletin of the Seismological Society of America*, v. 101, no. 4, p. 1542-1553.
- Nazareth, J.J. and Hauksson, E., 2004, The seismogenic thickness of the southern California crust: *Bulletin of the Seismological Society of America*, v. 94, no. 3, pp.940-960.
- NRC (U.S. Nuclear Regulatory Commission). 2012. Practical Implementation Guidelines for SSHAC Level 3 and 4 Hazard Studies. NUREG-2117, Rev. 1, Washington, D.C.
- Olson, B.P.E., 2015, Geomorphic evaluation of the Santa Monica Fault Zone, Northwestern Los Angeles Basin, Southern California, *Seismological Research Letters*, v. 86, no. 2B, p. 734.
- Page, M.T., Alderson, D. and Doyle, J., 2011, The magnitude distribution of earthquakes near Southern California faults: *Journal of Geophysical Research*, Vol. 116, B12309, doi:10.1029/2010JB007933.

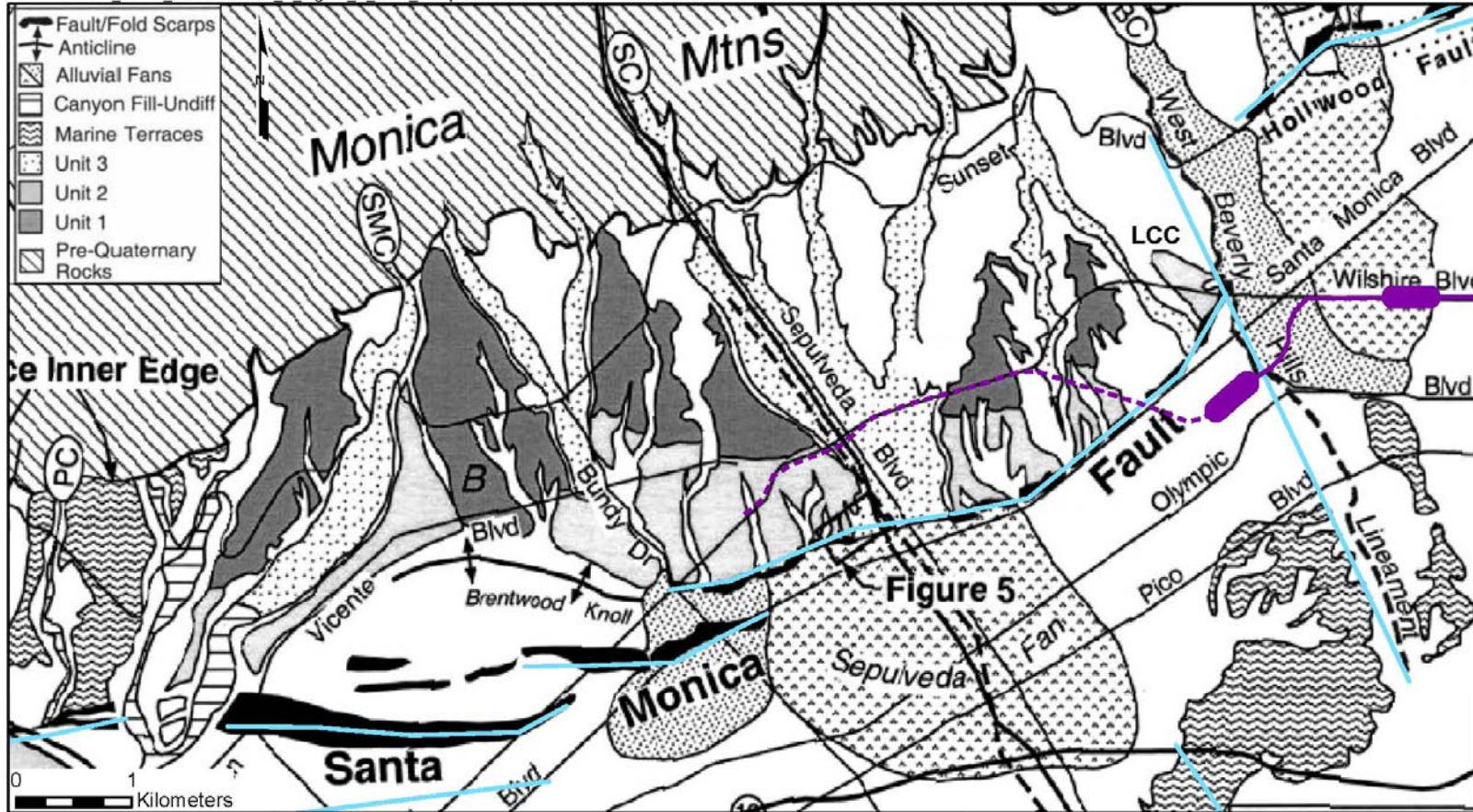
- Petersen, M.D., Frankel, A.D., Harmsen, S.C., Mueller, C.S., Haller, K.M., Wheeler, R.L., Wesson, R.L., Zeng, Y., Boyd, O.S., Perkins, D.M., Luco, N., Field, E.H., Wills, C.J., and Rukstales, K.S., 2008, Documentation for the 2008 Update of the United States National Seismic Hazard Maps: U.S. Geological Survey Open-File Report 2008–1128, 61 p.
- Petersen, M.D., Dawson, T.E., Chen, R., Cao, T., Wills, C.J., Schwartz, D.P., and Frankel, A.D., 2011, Fault displacement hazard for strike-slip faults: *Bulletin of the Seismological Society of America*, v. 101, no. 2, p. 805-825.
- Petersen, M.D., Moschetti, M.P., Powers, P.M., Mueller, C.S., Haller, K.M., Frankel, A.D., Zeng, Y., Rezaeian, S., Harmsen, S.C., Boyd, O.S., Field, Ned, Chen, R., Rukstales, K.S., Luco, N., Wheeler, R.L., Williams, R.A., and Olsen, A.H., 2014, Documentation for the 2014 update of the United States National Seismic Hazard Maps: U.S. Geological Survey Open-File Report 2014–1091, 243 p., <http://dx.doi.org/10.333/ofr20141091>
- Petersen, M.D., Zeng, Yuehua, Haller, K.M., McCaffrey, Robert, Hammond, W.C., Bird, Peter, Moschetti, Morgan, and Thatcher, Wayne, 2013, Geodesy- and geology-based slip-rate models for the Western United States (excluding California) national seismic hazard maps: U.S. Geological Survey Open-File Report 2013-1293, 80 p.
- Southern California Earthquake Data Center (SCEDC), 2016, Significant Earthquakes and Faults, Historical Earthquakes & Significant Faults in Southern CA: URL: <http://scedc.caltech.edu/significant/>; last visited on 25 January, 2016.
- Southern California Earthquake Data Center (SCEDC), 2016, Earthquake Catalogs: URL: <http://scedc.caltech.edu/eq-catalogs/index.html>; downloaded 25 January, 2016.
- Topozada, T.R., Bennett, J.H., Borchardt, G.A., Saul, R., and Davis, J.F., 1988, Planning Scenario for a Major Earthquake on the Newport–Inglewood Fault Zone: California Division of Mines and Geology Special Publication 99.
- Treiman, J., Hernandez, J, and Olson, B., 2015, Identifying Surface Rupture Hazard along the Northern Margin of the Los Angeles Basin: *Seismological Research Letters*, v. 86, no. 2B.
- Tsutsumi, H., Yeats, R.S., and Huftile, G.J., 2001, Late Cenozoic Tectonics of the Northern Los Angeles Fault System: *Geological Society of America Bulletin*, v. 113, no. 4, pp. 454-468.
- U.S. Geological Survey and California Geological Survey, 2010 (2014), Quaternary fault and fold database for the United States, accessed 2014, from USGS web site: <http://earthquake.usgs.gov/hazards/qfaults/>.
- Weaver, K.D., and Dolan, J.F., 2000, Paleoseismology and Geomorphology of the Raymond Fault, Los Angeles County, California: *Bulletin of the Seismological Society of America*, v. 90, no. 6, p. 1409-1429. doi: 10.1785/0119990075.
- Wells, D.L., and Coppersmith, K.J., 1994, New empirical relationships among magnitude, rupture length, rupture width, rupture area, and surface displacement: *Bulletin of the Seismological Society of America*, v. 84, no. 4, p. 974-1002.

- Wesnousky, S.G., 1986, Earthquakes, Quaternary faults, and seismic hazard in California: *Journal Geophysical Research*, v. 91, p. 2587–12631.
- Wesnousky, S.G., 2006, Predicting the endpoints of earthquake ruptures: *Nature*, v. 444, p. 358–360, doi:10.1038/nature05275.
- Wesnousky, S.G., 2008. Displacement and geometrical characteristics of earthquake surface ruptures: issues and implications for seismic-hazard analysis and the process of earthquake rupture.
- Wesnousky, S.G., and Biasi, G.P., 2011, The length to which an earthquake will go to rupture: *Bulletin of the Seismological Society of America*, v.101, p. 1948-1950.
- Working Group on California Earthquake Probabilities (WGCEP), 2008, The Uniform California Earthquake Rupture Forecast, Version 2 (UCERF 2): U.S. Geological Survey Open-File Report 2007-1437 and California Geological Survey Special Report 203 [<http://pubs.usgs.gov/of/2007/1437/>].
- Wright, T.L., 1991, Structural geology and tectonic evolution of the Los Angeles basin: in Biddle, K.T., ed., *Active Margin Basins*, American Association of Petroleum Geologists Memoir 52, p. 35-134.
- Youngs, R.R., and Coppersmith, K.J., 1985, Implications of fault slip rates and earthquake recurrence models to probabilistic seismic hazard estimates: *Bulletin of the Seismological Society of America*, v. 75, no. 4, p. 939-964.
- Youngs, R.R., Arabasz, W.J., Anderson, R.E., Ramelli, A.R., Ake, J.P., Slemmons, D.B., McCalpin, J.P., Doser, D.I., Fridrich, C.J., Swan, F.H. III, Rogers, A.M., Yount, J.C., Anderson, L.W., Smith, K.D., Bruhn, R.L., Knuepfer, L.K., Smith, R.B., dePolo, C.M., O’Leary, K.W., Coppersmith, K.J., Pezzopane, S.K., Schwartz, D.P., Whitney, J.W., Olig, S.S., and Toro G.R., 2003, A methodology for probabilistic fault displacement hazard analysis (PFDHA), *Earthquake Spectra*, v. 19, no. 1, p. 191-219.
- Ziony, J.I., ed., 1985, *Evaluating Earthquake Hazards in the Los Angeles Region—An Earth Science Perspective*, U.S. Geological Survey Professional Paper 1360.

APPENDIX A FIGURES

Figure 1: Quaternary Faults and Geomorphic Features

S:\OD15\4953 Metro Westside\sect 2 Figure 1 SMF scarps.mxd



Legend

- Purple Line Extension (Section 2 solid; Section 3 dashed)
- Quaternary Faults (USGS, 2014)

Base Map from Dolan et al. (2000)

PC - Potrero Canyon; BC - Benedict Canyon;
 SC - Sepulveda Canyon; SMC - Santa Monica
 Canyon; LCC - Los Angeles Country Club

QUATERNARY FAULTS AND
 GEOMORPHIC FEATURES
 Fault Displacement Hazard Evaluation
 Westside Purple Line Extension -
 Section 2
 Beverly Hills, California

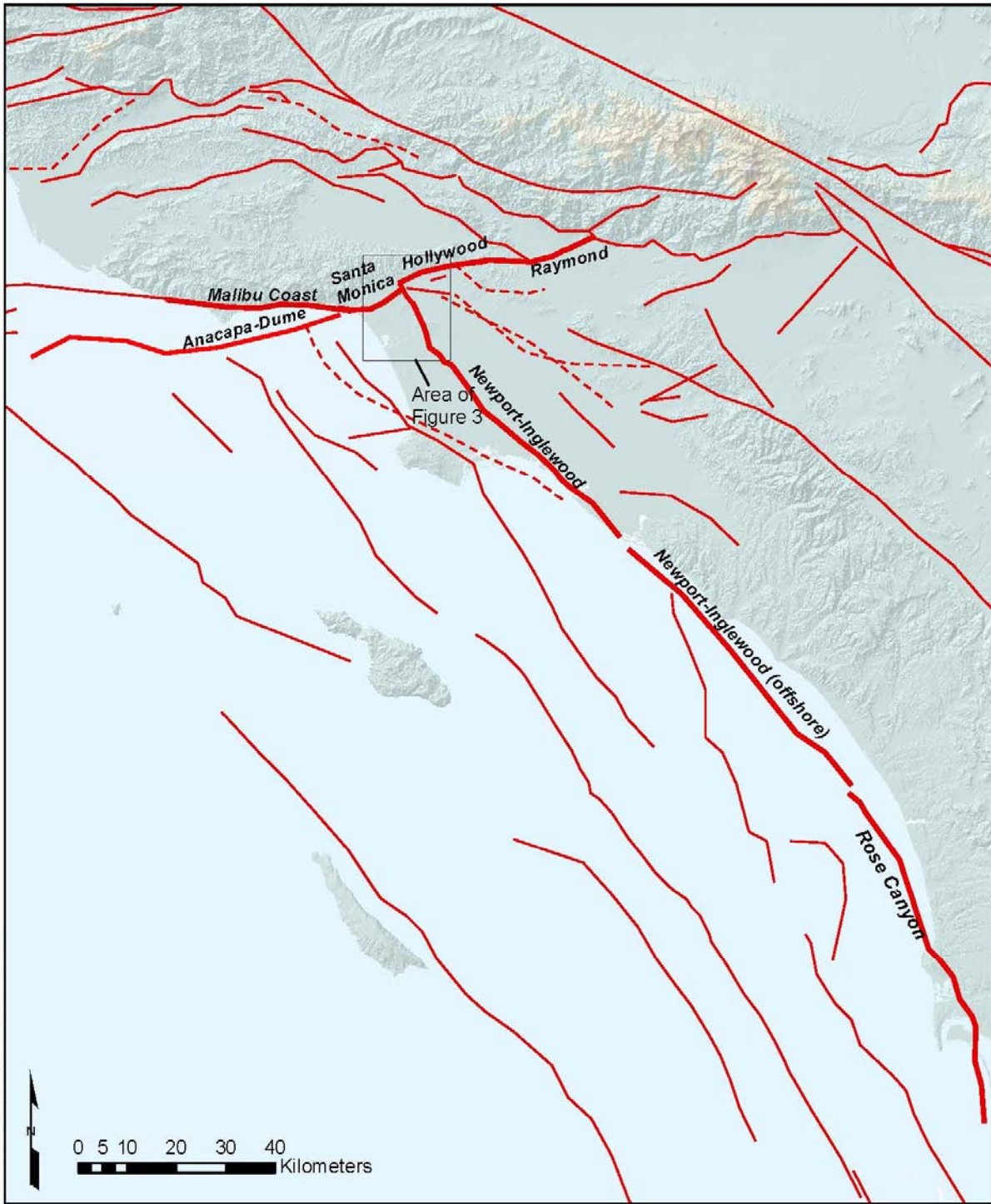


Figure
1

Date: 02/24/2017


Project No. 4953111423.21.01

Figure 2: Regional Extent of Fault Sources



S:\OD15\4953_Metro_Westside\sect_2_Figure_2_faults_regional.mxd

Legend

 UCERF3 FM 3.1 - Modeled Traces dashed where buried, thick lines for faults modeled in PFDHA (Field et al., 2013)

REGIONAL EXTENT OF
FAULT SOURCES
Fault Displacement Hazard Evaluation
Westside Purple Line Extension -
Section 2
Beverly Hills, California

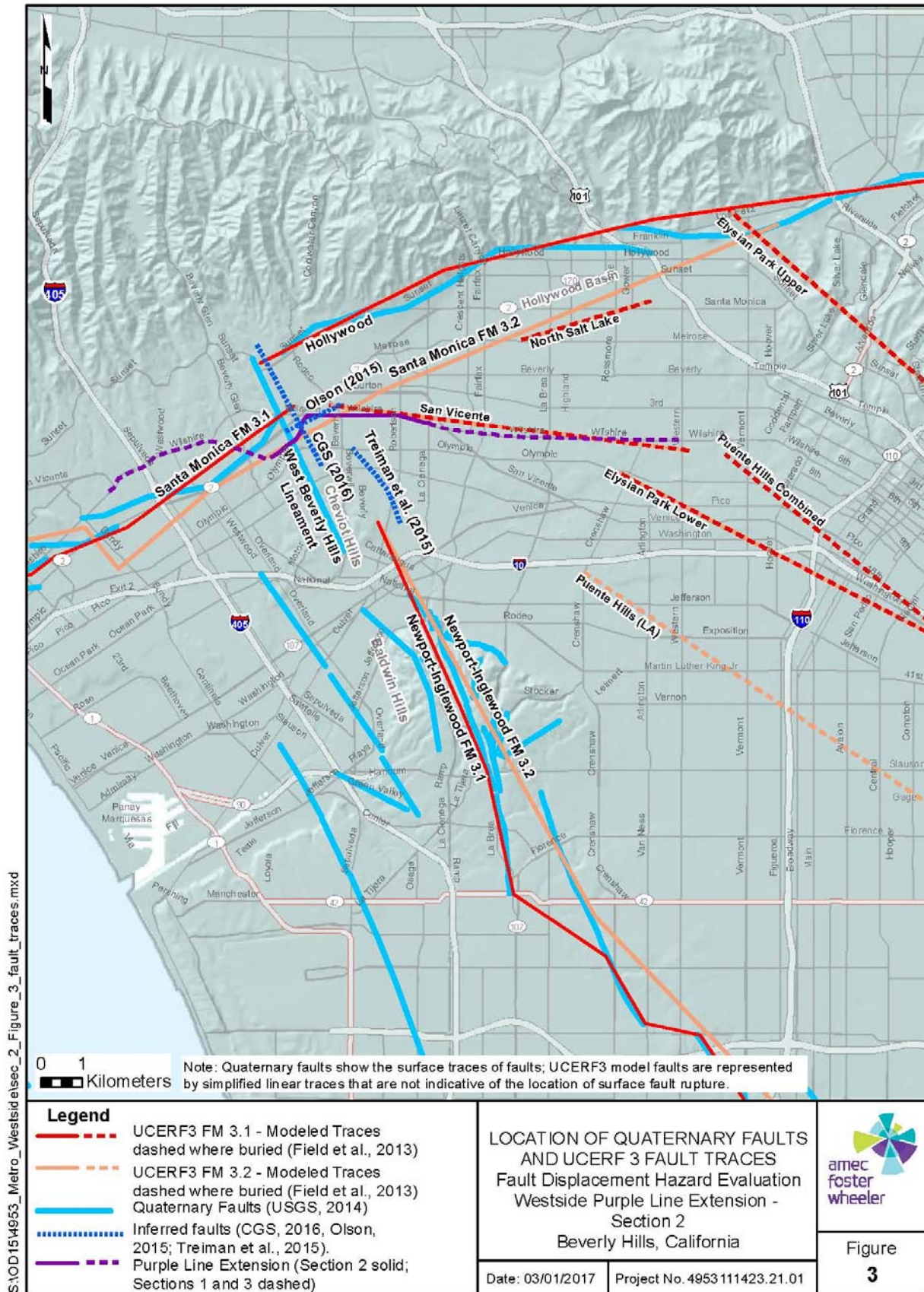


Figure
2

Date: 02/24/2017

Project No. 4953111423.21.01

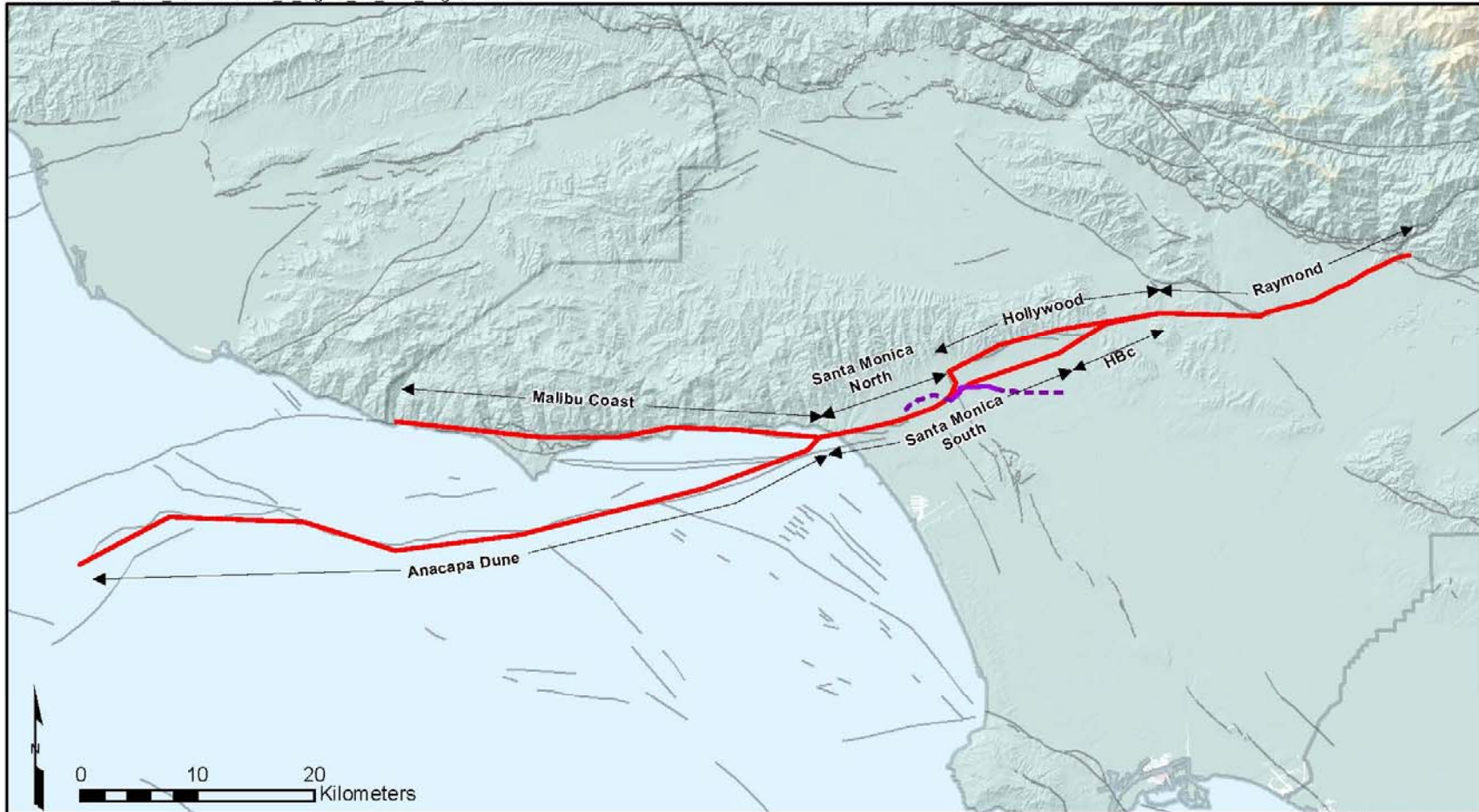
Figure 3: Location of Quaternary Faults and UCERF 3 Fault Traces



S:\OD1514953_Metro_Westside\sec_2_Figure_3_fault_traces.mxd

Figure 4: Fault Segments for Santa Monica Fault Rupture Scenarios

S:\OD15\4953 Metro Westside\sect 2 Figure 04 fault segments.mxd



Legend

- Fault Segments; Hbc is Hollywood Basin connector to Raymond
- Quaternary Faults (USGS, 2014)
- - - Purple Line Extension (Section 2 solid; Sections 1 and 3 dashed)

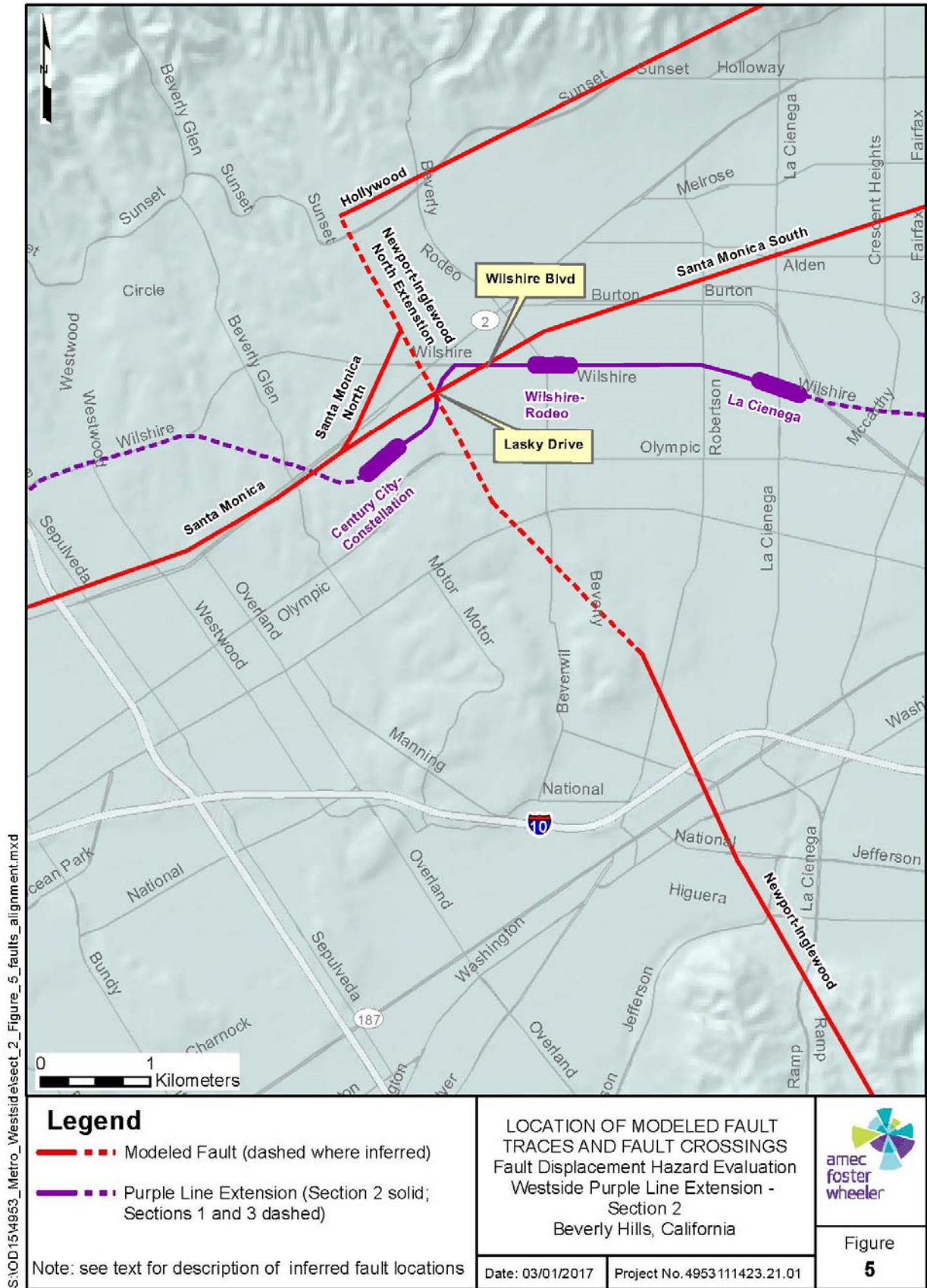
FAULT SEGMENTS FOR SANTA MONICA FAULT RUPTURE SCENARIOS
 Fault Displacement Hazard Evaluation
 Westside Purple Line Extension - Section 2
 Beverly Hills, California



Date: 02/24/2017 Project No. 4953111423.21.01

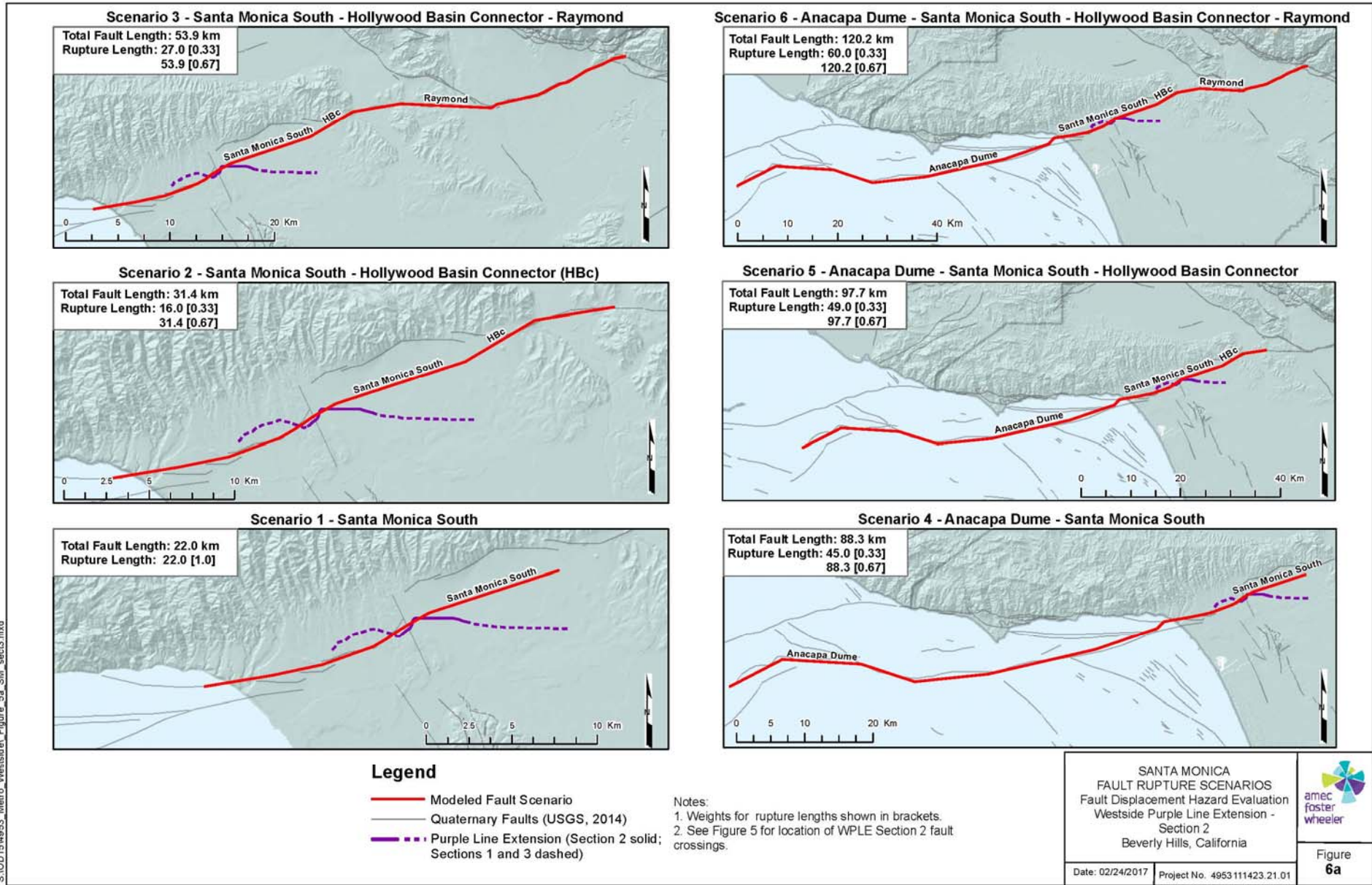
Figure 4

Figure 5: Location of Modeled Fault Traces and Fault Crossings



S:\0154953_Metro_Westside\sect_2_Figure_5_faults_alignment.mxd

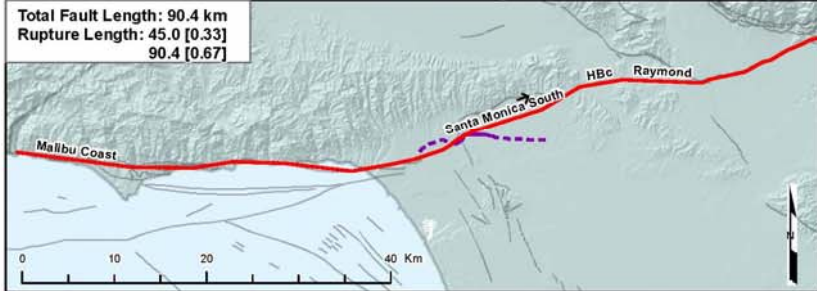
Figure 6: Santa Monica Fault Rupture Scenarios



S:\OD\154963_Metro_Westside\Figure_5a_SM_sect3.mxd

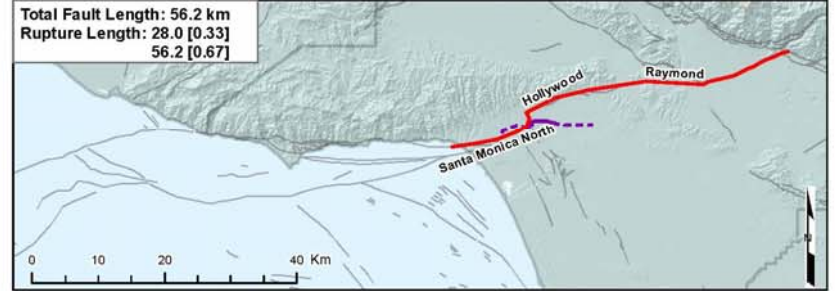
Scenario 9 - Malibu Coast - Santa Monica South - Hollywood Basin Connector - Raymond

Total Fault Length: 90.4 km
 Rupture Length: 45.0 [0.33]
 90.4 [0.67]



Scenario 12 - Santa Monica North - Hollywood - Raymond

Total Fault Length: 56.2 km
 Rupture Length: 28.0 [0.33]
 56.2 [0.67]



Scenario 8 - Malibu Coast - Santa Monica South - Hollywood Basin Connector (HBC)

Total Fault Length: 67.9 km
 Rupture Length: 34.0 [0.33]
 67.9 [0.67]



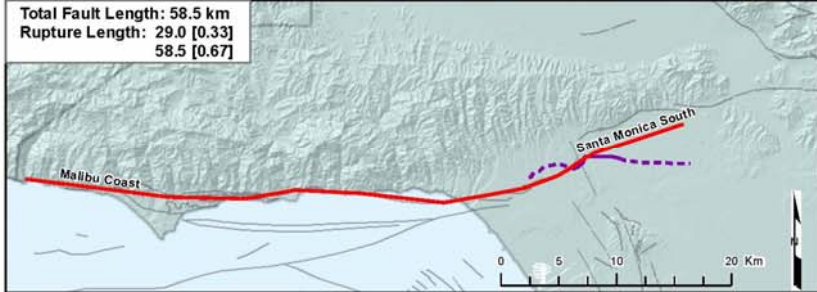
Scenario 11 - Santa Monica North - Hollywood

Total Fault Length: 33.7 km
 Rupture Length: 17.0 [0.33]
 33.7 [0.67]



Scenario 7 - Malibu Coast - Santa Monica South

Total Fault Length: 58.5 km
 Rupture Length: 29.0 [0.33]
 58.5 [0.67]



Scenario 10 - Santa Monica North

Total Fault Length: 12.8 km
 Rupture Length: 12.8 [1.0]



Legend

- Modeled Fault Scenario
- Quaternary Faults (USGS, 2014)
- - - Purple Line Extension (Section 2 solid; Sections 1 and 3 dashed)

Notes:
 1. Weights for rupture lengths shown in brackets.
 2. See Figure 5 for location of WPLE Section 2 fault crossings.

SANTA MONICA FAULT RUPTURE SCENARIOS Fault Displacement Hazard Evaluation Westside Purple Line Extension - Section 2 Beverly Hills, California		 amec foster wheeler
Date: 02/24/2017	Project No. 4953111423.21.01	

Figure 6b

Scenario 15 - Anacapa Dume - Santa Monica North - Hollywood - Raymond



Scenario 18 - Malibu Coast - Santa Monica North - Hollywood - Raymond



Scenario 14 - Anacapa Dume - Santa Monica North - Hollywood



Scenario 17 - Malibu Coast - Santa Monica North - Hollywood



Scenario 13 - Anacapa Dume - Santa Monica North



Scenario 16 - Malibu Coast - Santa Monica North



Legend

- Modeled Fault Scenario
- Quaternary Faults (USGS, 2014)
- - - Purple Line Extension (Section 2 solid; Sections 1 and 3 dashed)

Notes:

1. Weights for rupture lengths shown in brackets.
2. See Figure 5 for location of WPLE Section 2 fault crossings.

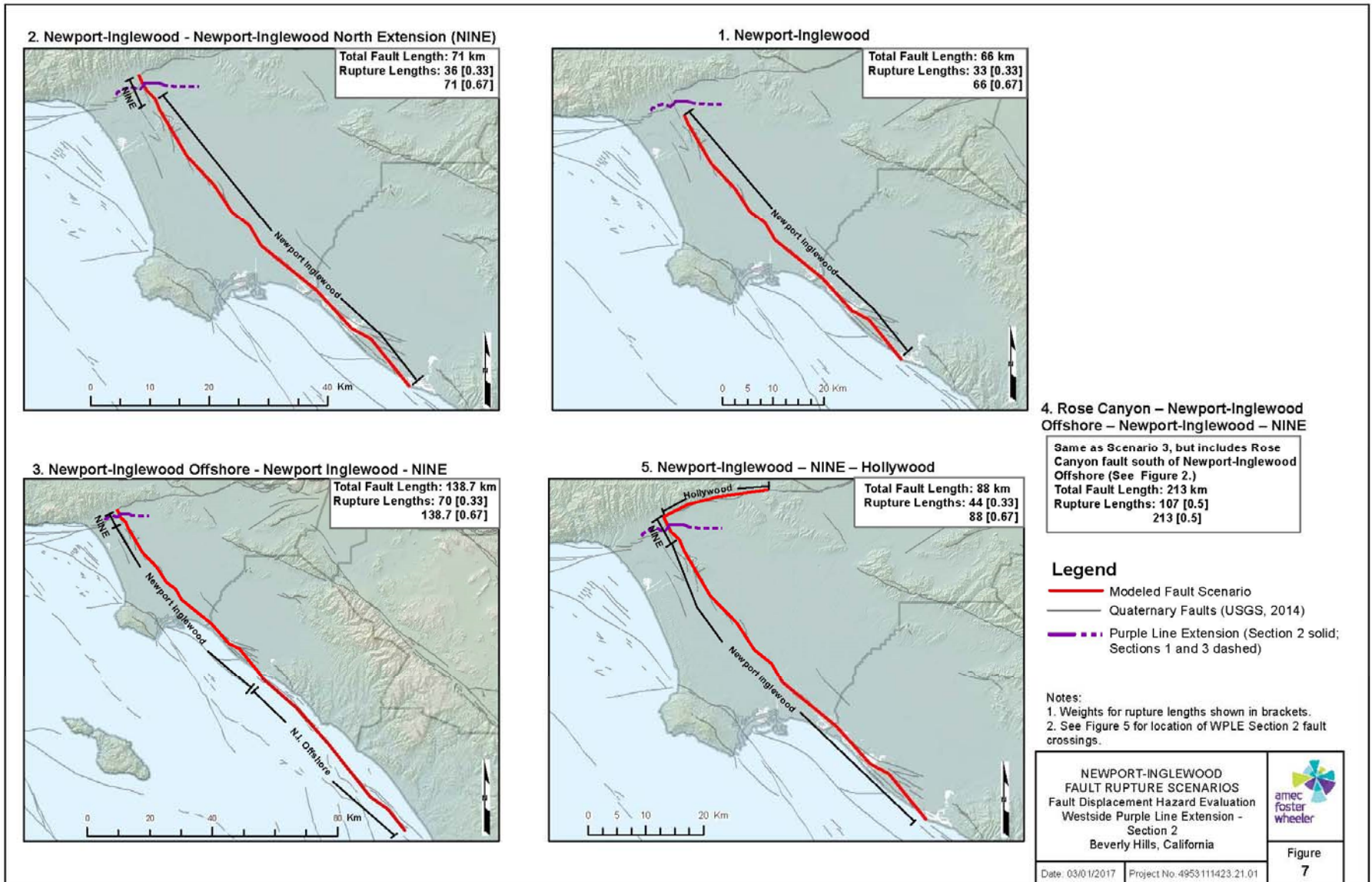
SANTA MONICA
FAULT RUPTURE SCENARIOS
Fault Displacement Hazard Evaluation
Westside Purple Line Extension -
Section 2
Beverly Hills, California



Date: 02/24/2017 Project No. 4953111423.21.01

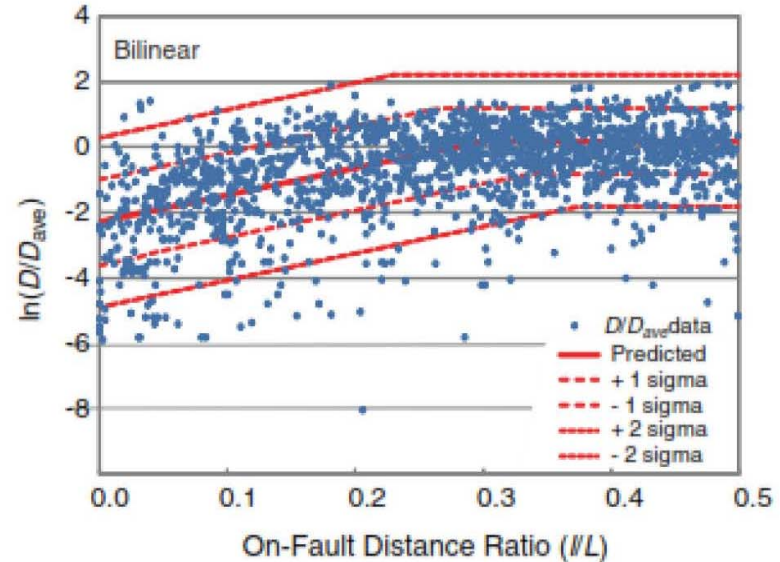
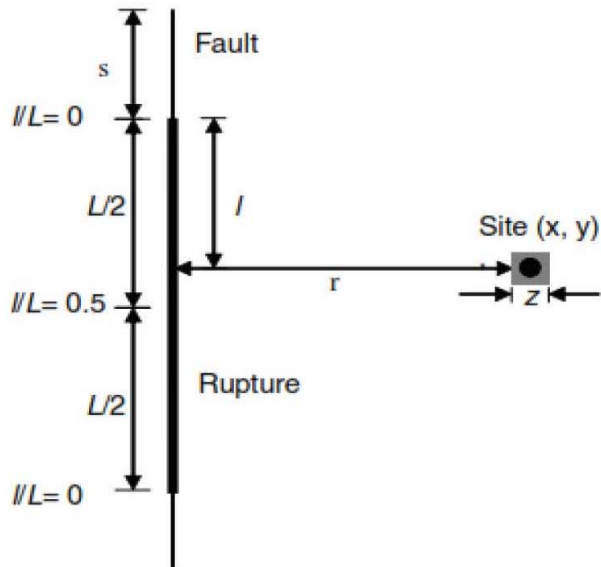
Figure
6c

Figure 7: Newport-Inglewood Fault Rupture Scenarios



S:\015\4953_Metro_Westside\elect_2\Figure_7_NI_FaultRuptureScenario.mxd

Figure 8: Geometry and Displacement Model for Strike-Slip Faulting



A. Definitions of variables for PFDHA: x and y are site coordinates; z is dimension of the area considered for calculating the probability of fault rupture (area z^2); r is distance from the site to the mapped fault trace; l/L is on-fault distance ratio, where l is distance measured from the nearest point on the rupture to the closest end of the rupture and L is total rupture length; and s is distance from the end of the rupture to the end of the fault.

B. Bi-linear regression model for normalized principal fault displacement $[\ln(D/D_{ave})]$ versus on-fault displacement ratio $[l/L]$.

Note: Modified from Petersen et al., 2011

GEOMETRY AND DISPLACEMENT
MODEL FOR STRIKE-SLIP FAULTING
Fault Displacement Hazard Evaluation
Westside Purple Line Extension -
Section 2
Los Angeles, California



Figure
8

Date: 02/23/2017

Project No. 4953111423.21.01

Figure 9: Santa Monica rupture Scenario Contributions and Total Mean Displacement Hazard

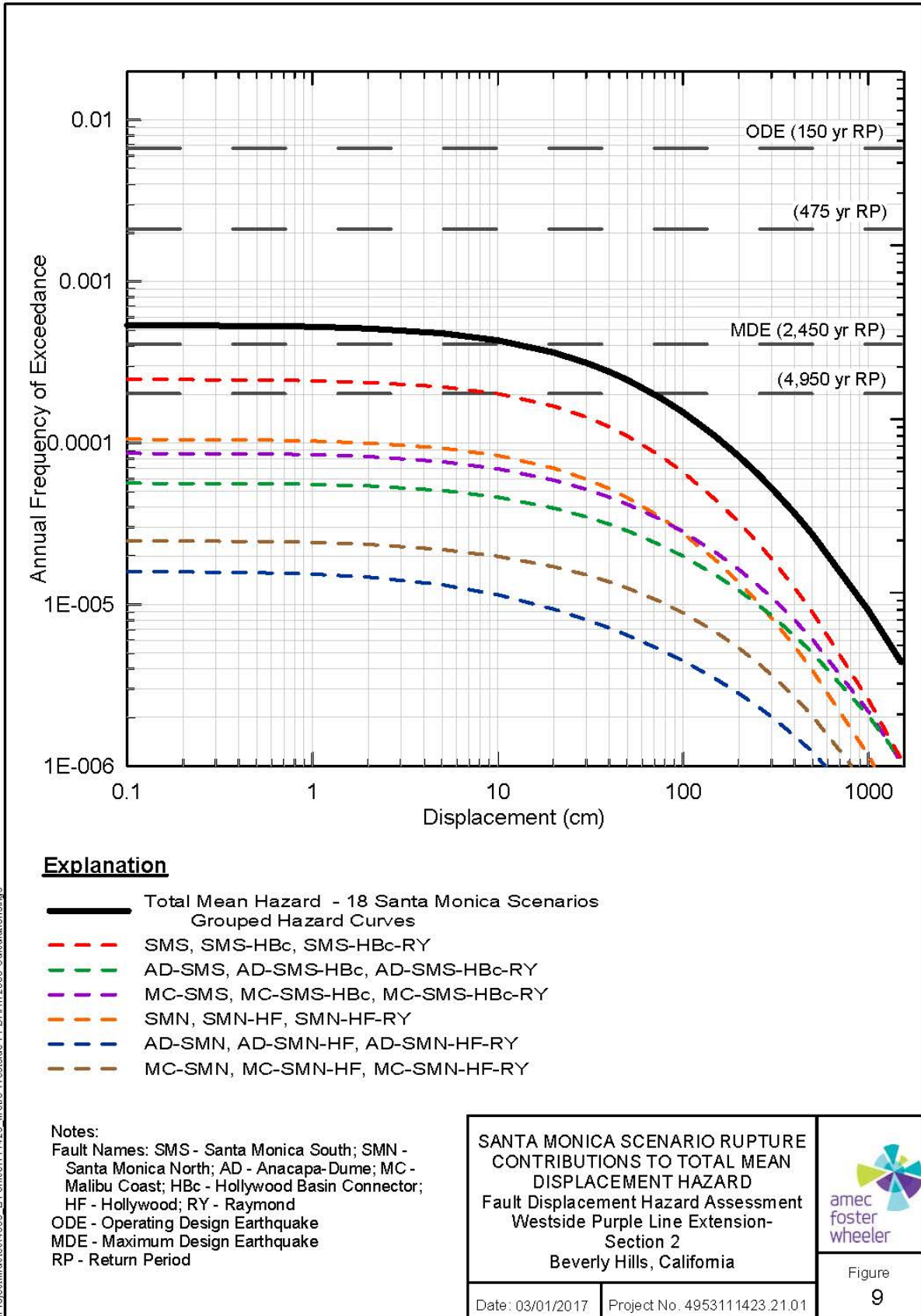
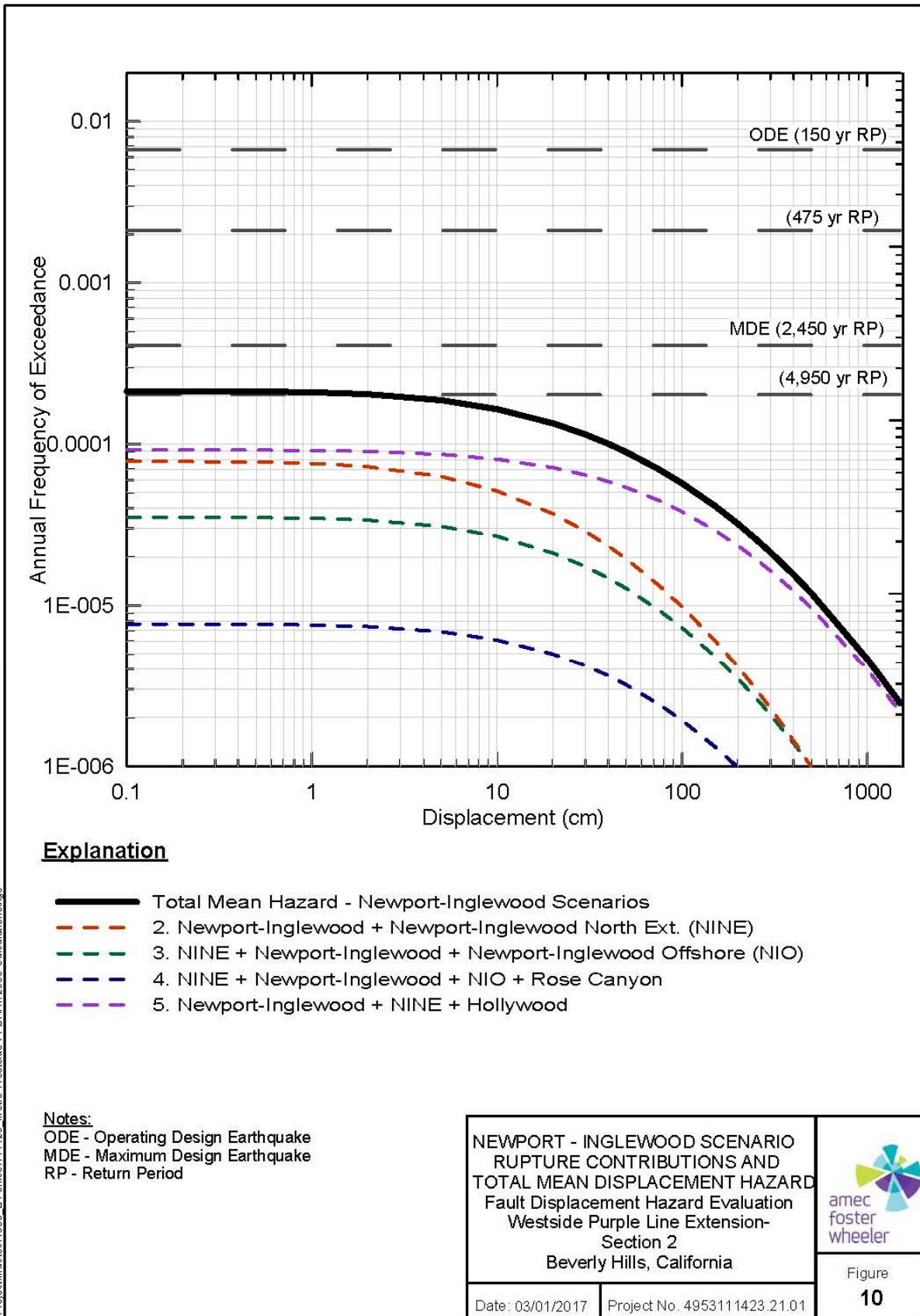


Figure 10: Newport-Inglewood Rupture Scenario Contributions and Total Mean Displacement Hazard



I:\Project\4953_LA_office\111423_Metro Westside PFD\HA1 2000 Calculations\figs